STOKES' PROBLEM FOR

THE

INFINITE ROD

By

JOHN EDWARD KIPP

Bachelor of Science
University of Kansas
Lawrence, Kansas
1951

Master of Science
University of Kansas
Lawrence, Kansas
1955

Submitted to the Faculty of the Graduate School
of the Oklahoma State University
in partial fulfillment of the requirements
for the degree of
DOCTOR OF PHILOSOPHY
July 31, 1968

STOKES' PROBLEM FOR

THE

INFINITE ROD

Thesis Approved:

Gerald D Parker

Thesis Adviser

Kenneth J Bell

Donald E. Boyd

D. M. MacAlpine

D. D. Durham

Dean of the Graduate School

ACKNOWLEDGEMENT

I gratefully acknowledge the assistance of the following individuals and groups:

Dr. J. D. Parker, who served as my thesis advisor. His patience and wise counsel during the course of my graduate study at Oklahoma State University was invaluable.

My graduate committee, the members of which were Dr. D. M. MacAlpine, Dr. D. G. Boyd, and Dr. K. J. Bell.

The National Science Foundation for financial support.

TABLE OF CONTENTS

LIST OF TABLES

LIST OF FIGURES

NOTATION

Symbols are defined throughout the text as they are used to describe physical or mathematical quantities. The most important symbols and the quantities they represent are as follows:

α . . . . Constant

ω . . . . Rod Oscillation Frequency

ν . . . . Kinematic Viscosity

μ . . . . Dynamic Viscosity

ρ . . . . Fluid Density

ρ_f . . . . Viscosimeter Float Density

a . . . . Rod Oscillation Amplitude

p . . . . Pressure also $\left(\frac{\rho\alpha}{\mu} \right)^{\frac{1}{2}}$

r . . . . Radial Distance

R . . . . Rod Radius

t . . . . Time

u . . . . Radial Velocity Component

U_o . . . . Maximum Rod Velocity

v . . . . Tangential Velocity Component

w . . . . Axial Velocity Component

CHAPTER I

Introduction

1-1. Statement of the Problem

The primary purpose of this study is to extend the state of knowledge of time-dependent laminar flows to include an axisymmetric flow. In particular, this study will inquire, both theoretically and experimentally, into the velocity field induced in an infinite body of an incompressible viscous fluid by the harmonic axial oscillation of an infinitely long cylinder within the fluid. The corresponding problem for a flat plate is frequently described as Stokes' problem; in view of this, it seems fitting to consider this as an extension of the Stokes' problem to include the infinite cylinder.

Any engineering investigation should be motivated by more than just the pursuit of knowledge per se; in other words, a requirement should exist for the information which is derived from the research. In this particular case, bodies of cylindrical cross sections frequently, by design or otherwise, are subjected to harmonic axial oscillations. To predict the effect that such motion may have upon the heat, momentum or mass transfer to or from the oscillating body, knowledge of the velocity field about the body is required. Since, as will be shown, such information does not seem to be available, it was felt that this study would prove useful to the engineering and scientific community. In addition to the value to be derived from this study by those individuals working in related areas, the results of this study will also make available the detailed information regarding the laminar flow field which might be necessary for further studies in flow instability and transition to turbulence. Finally, the studies described herein will indicate if significant deviations result when a finite flow system is used as a model to study experimentally an idealized infinite flow system.

1-2. Literature Review

Schlichting (23)* has indicated that the basic differential equations describing the flow of a viscous fluid, the Navier-Stokes equations, were first developed by M. Navier in 1827, the development being based upon the consideration of intermolecular forces. In 1843, B. de Saint Venant, and in 1845, G. G. Stokes, developed the same equations based upon an assumed linearity of normal and shearing stresses with respect to the rate of deformation. While Bateman (3) has indicated that many authors have questioned the validity of the Navier-Stokes equations, the close agreement achieved when the theoretical solutions obtained from these equations are compared with experimental data for parallel flows, in particular flows in circular ducts and flows between rotating concentric cylinders, has led to general acceptance of the validity of the Navier-Stokes equations.

In 1851, G. G. Stokes (26) presented solutions to two unsteady parallel flow problems in his discussion of the motion of pendulums. A solution for the velocity profile induced in the fluid was presented for the case where an infinite flat plate submerged in a viscous medium was suddenly given a velocity U_o in a direction parallel

---

*Numbers in parentheses refer to references in the Bibliography.

the plate. The solution obtained was of the form

$$u(y,t) = U_o \operatorname{erfc} \frac{y}{2(\frac{\mu t}{\rho})^{1/2}} \qquad (1\text{-}2.1)$$

This sort of problem is also frequently described in the literature as an "indicial" problem. While this solution was first given by Stokes, in 1911 Lord Rayleigh (23) presented a similar solution for the same problem. It is now most common in the literature to find any such indicial problem described as a "Rayleigh Problem". The second solution which Stokes presented was again for a velocity profile induced in an infinite body of a viscous medium when an infinite flat plate submerged therein was given a particular motion (in this case a harmonic oscillation) parallel to itself. The solution obtained was of the form

$$u(y,t) = U_o \exp\left(-(\frac{\omega}{2\nu})^{1/2} t\right) \cos\left(\omega t - (\frac{\omega}{2\nu})^{1/2} y\right) \qquad (1\text{-}2.2)$$

This latter problem is now most frequently described as "Stokes' Problem", but at least one author, Schlichting (23), describes this as "Stokes' Second Problem".

Many extensions of the time-dependent flat plate solutions have been discussed. For the most part, these studies have been concerned with the Rayleigh problem. Watson (27) showed that similar solutions could be obtained for the indicial problem not only for the case already discussed where the plate is given a constant velocity U_o, but also for

$$U(t) = At^{\alpha} \qquad (1\text{-}2.3)$$

$$U(t) = Ae^{ct} \qquad (1\text{-}2.4)$$

where A, C, and α are constants. Hasimoto (7) extended the indicial problem to include a wedge (formed by the intersection of two semiinfinite planes) moving parallel to its edge. Glauert (6) applied an iterative technique to obtain a solution for a stagnation flow against a flat plate undergoing harmonic oscillations in its own plane. In this same connection, Wuest (29) considered a similar problem for the motion of an infinite cylinder in cross flow subjected to an axial motion.

For the infinite cylinder undergoing motion parallel its own longitudinal axis, where submerged in a viscous medium, the available literature is limited. No references were found which considered Stokes' problem. The Rayleigh problem was studied by Batchelor (1) and by Hasimoto (9). Batchelor obtained a solution, for the indicial parallel flow, for both the induced velocity profile as well as the viscous drag on the cylinder. Hasimoto extended this work to include cylinders of arbitrary cross section.

There were no experimental studies of induced velocity profiles in the literature for either the Rayleigh problem or Stokes' problem for the flat plate. O'Brien and Logan (18), in 1964, studied experimentally the flow induced in a viscous fluid between two infinite flat plates when one was oscillated harmonically in its own plane. By photographing a dye trace, they were able to obtain displacement profiles for a problem closely related to Stokes' problem. Their results confirm the theoretical analysis, that such a flow is essentially a composite flow made up of a zero pressure gradient oscillatory flow and pulsating channel flow.

No experimental studies were reported in the literature for either the indicial problem or Stokes' problem for an infinite cylinder.

While there are a number of studies of the stability of steady laminar flows, as well as the associated problem of transition to a turbulent flow, none specifically deal with these aspects of this investigation. Lin's paper (15) gives an introduction to the theoretical aspects of hydrodynamic stability. However, there is little discussion of the problem with respect to time-dependent flows. While not directly concerned with the oscillating rod, mention should be made of Li's study (14) of the transition of the flow induced by the oscillation of a plate in a viscous medium, since this investigation did yield a critical Reynolds number for transition to turbulence $\frac{\omega^{\frac{1}{2}} d}{\nu^{\frac{1}{2}}}$ of 800, where ω is the oscillation frequency, and d is the total rod displacement. In addition, the more recent works of Sarpkaya (21) and Combs and Gilbrech (2), which deal with pulsating viscous flow in circular tubes, also provide additional insight into the hydrodynamic stability problem.

Studies bearing upon the experimental portion of this study have been presented by a number of authors. A paper by Grant and Kronauer (7) was found to provide a brief survey of the basic principles of hot wire anemometry. Runstadler (20) has outlined a number of problems which have appeared as a consequence of the use of hot wire and hot film anemometers in liquids. Wills (28) has determined corrections for hot wire readings taken in the proximity of a solid boundary

CHAPTER II

Theoretical Considerations

2-1. Equations of Motion

The theoretical aspect of this study was directed toward obtaining a solution to the Navier-Stokes Equations

$$\frac{\partial u}{\partial t} + \frac{u\partial u}{\partial r} + \frac{v}{r}\frac{\partial u}{\partial \theta} + w\frac{\partial u}{\partial z} - \frac{v^2}{r}$$

$$= -\frac{1}{\rho}\frac{\partial p}{\partial r} + \nu[\nabla^2 u - \frac{u}{r^2} - \frac{2}{r^2}\frac{\partial v}{\partial \theta}], \qquad (2\text{-}1.1)$$

$$\frac{\partial v}{\partial t} + \frac{u\partial v}{\partial r} + \frac{v}{r}\frac{\partial v}{\partial \theta} + w\frac{\partial v}{\partial z} + \frac{uv}{r}$$

$$= -\frac{1}{\rho r}\frac{\partial p}{\partial \theta} + \nu[\nabla^2 v + \frac{2}{r^2}\frac{\partial u}{\partial \theta} - \frac{v}{r^2}], \qquad (2\text{-}1.2)$$

$$\frac{\partial w}{\partial t} + \frac{u\partial w}{\partial r} + \frac{v}{r}\frac{\partial w}{\partial \theta} + \frac{w\partial w}{\partial z}$$

$$= -\frac{1}{\rho}\frac{\partial p}{\partial z} + \nu\nabla^2 w, \qquad (2\text{-}1.3)$$

subject to the boundary conditions

$$w(R,t) = U_o \cos \omega t, \qquad (2\text{-}1.4)$$

and

$$w(\infty,t) = 0 . \qquad (2\text{-}1.5)$$

It should be noted that in the derivation of these equations of motion it was assumed that the flow was isothermal, all fluid properties were constant, and that the fluid was Newtonian.

Figure 1 shows the system used in the following analysis.

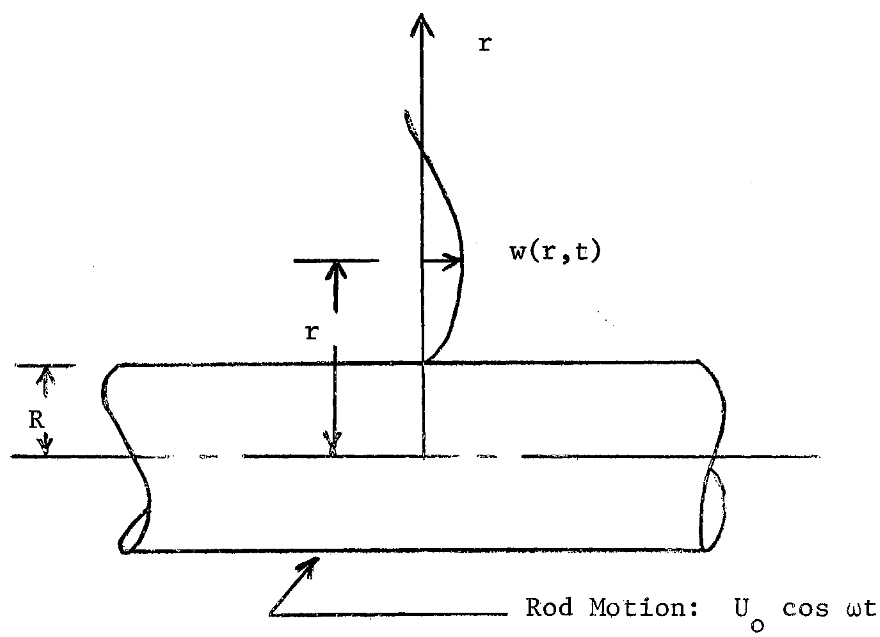

Figure 1. System for theoretical analysis

To make the problem more tractable, it was decided to limit this investigation to the case where the only fluid velocity which would be admitted would be the axial component parallel to the oscillating rod. The tangential and radial velocity components were defined to be identically zero. A consequence of these assumptions, was the reduction of the Navier-Stokes Equations to a single linear partial differential equation

$$\frac{\partial w}{\partial t} = \nu \nabla^2 w \tag{2-1.6}$$

Equations (2-1.4) and (2-1.5) remain unchanged.

In passing it should be noted that a solution for the differential system described above is said to be an exact solution, since no terms in the equations of motion have been neglected because they were small when compared with other terms of the differential equation.

2-2. Solution of the Equations of Motion

The equation of motion, in the axial direction, may be written in cylindrical coordinates

$$\frac{\partial w}{\partial t} = \frac{\mu}{\rho} \left(\frac{\partial^2 w}{\partial r^2} + \frac{1}{r} \frac{\partial w}{\partial r} \right) \tag{2-2.1}$$

Frequently, linear partial differential equations of the above form may have a solution

$$w(r,t) = F(r) \cdot T(t). \tag{2-2.2}$$

If a solution of this form is assumed and is substituted in the equation of motion, two ordinary differential equations result. These are

$$T' - i\alpha T = 0, \tag{2-2.3}$$

and

$$\frac{F''}{F} + \frac{1}{r}\frac{F'}{F} - \frac{i\rho\alpha}{\mu} = 0, \qquad (2\text{-}2.4)$$

where α is a real constant.

Equation (2-2.3) yields

$$T = e^{i\alpha t} \qquad (2\text{-}2.5)$$

while equation (2-2.4) yields either

$$R = AJ_o\,((\frac{-i\rho\alpha^{\frac{1}{2}}r}{\mu}) + BY_o(\frac{i\rho\alpha^{\frac{1}{2}}r}{\mu}) \qquad (2\text{-}2.6)$$

or

$$R = CI_o\,(\frac{i\rho\alpha^{\frac{1}{2}}r}{\mu}) + DK_o(\frac{i\rho\alpha^{\frac{1}{2}}r}{\mu}) \qquad (2\text{-}2.7)$$

It is usual to use a composite solution

$$R = AJ_o\,(i^{3/2}r) + BK_o(i^{\frac{1}{2}}pr) \qquad (2\text{-}2.8)$$

where

$J_o(i^{3/2}pr)$ = zeroth order modified Bessel function of the first kind,

$K_o(i^{1/2}pr)$ = zeroth order modified Bessel function of the second kind

and $p = (\frac{\rho\alpha}{\mu})^{1/2}$.

Then

$$w\,(r,t) = e^{i\alpha t}\,[\,AJ_o(i^{3/2}pr) + BK_o(i^{1/2}pr)\,]. \qquad (2\text{-}2.9)$$

Since a solution is desired only outside a cylinder of radius R, the behavior of the solution at r = 0 is of no concern. However, since

$$w(\infty,t) = 0, \qquad (2\text{-}2.10)$$

the behavior of $J_o(i^{3/2}pr)$ and $K_o(i^{1/2}pr)$,

as r becomes large, is of consequence. A conventional representation of these functions is

$$J_o(i^{3/2}pr) = \text{ber } pr + i \text{ bei } pr,$$

and

$$K_o(i^{1/2}pr) = \text{ker } pr + i \text{ kei } pr.$$

The ber, bei, ker, and kei functions are usually known as Thompson (or Kelvin) functions and have asymptotic approximations for large values of x.

$$\text{ber } x \approx \frac{1}{\sqrt{2\pi x}} [\exp(\frac{x}{\sqrt{2}})] \cos(\frac{x}{\sqrt{2}} - \frac{\pi}{8}) \quad (2\text{-}2.11)$$

$$\text{bei } x \approx \frac{1}{\sqrt{2\pi x}} [\exp(\frac{x}{\sqrt{2}})] \sin(\frac{x}{\sqrt{2}} - \frac{\pi}{8}) \quad (2\text{-}2.12)$$

$$\text{ker } x \approx [\frac{\pi}{2x}]^{\frac{1}{2}} [\exp(\frac{-x}{\sqrt{2}})] \cos(\frac{x}{\sqrt{2}} + \frac{\pi}{8}) \quad (2\text{-}2.13)$$

$$\text{kei } x \approx [\frac{\pi}{2x}]^{\frac{1}{2}} [\exp(\frac{-x}{\sqrt{2}})] \sin(\frac{x}{\sqrt{2}} + \frac{\pi}{8}) \quad (2\text{-}2.14)$$

If w (r,t) is to converge to zero as r becomes large, in view of the above expressions, the coefficient of $J_o(i^{3/2}pr)$ must be zero. The solution to the equation of motion may then be written

$$w(r,t) = Be^{i\alpha t} K_o(i^{1/2}pr). \quad (2\text{-}2.15)$$

At $r = R$,

$$w(R,t) = U_o \cos \omega t, \tag{2-2.16}$$

hence

$$U_o \cos \omega t = B(\cos \alpha t + i \sin \alpha t) \; K_o(i^{1/2} pR), \tag{2-2.17}$$

so that

$$\alpha = \omega,$$

and

$$B = \frac{U_o}{D},$$

where

$$D = K_o \, (i^{1/2} pR).$$

Therefore,

$$w(r,t) = \frac{U_o}{D} \left(K_o(i^{1/2} pr) \right) e^{i\omega t} \tag{2-2.18}$$

or

$$\frac{w}{U_o}(r,t) = \frac{K_o(i^{1/2} pr)}{K_o(i^{1/2} pR)} e^{i\omega t} . \tag{2-2.19}$$

Since

$$K_o(i^{1/2} pr) = \text{ker } pr + i \text{ kei } pr$$

equation (2-2.19) may be written

$$\frac{w}{U_o} = \frac{(\cos \omega t + i \sin \omega t) \; (\text{ker } pr + i \text{ kei } pr)}{\text{ker } pR + i \text{ kei } pR} \tag{2-2.20}$$

If equation (2-2.20) is rationalized, the resulting expression is

$$\frac{w}{U_o} = \frac{1}{\text{ker}^2 \; pR + \text{kei}^2 \; pr} \Big((\text{ker } pr \text{ kei } pR + \text{kei } pr \text{ kei } pR) \cos\omega t$$

$$- (\text{kei } pr \text{ kei } pR - \text{ker } pr \text{ kei } pR) \sin \omega t \Big) . \tag{2-2.21}$$

Figure 2 portrays graphically the velocity profile induced in the fluid for the instant of maximum rod velocity, $\omega t = 0$, as well as the profile a quarter cycle later, $\omega t = \pi/2$. Profiles during the second quarter cycle will produce symmetry about the line $u/U = 0$. As one might expect, the induced profiles are quite similar in appearance to those which would be obtained from a study of the oscillating flat plate, and they clearly show the propagation of the shear wave radially outward from the oscillating rod. While there are inflection points in the induced profiles, the fluid velocities in the neighborhood of these inflection points is considerably less than experienced by the fluid in close proximity to the rod. In general, breakdown of the laminar flow and transition to turbulence, if it occurs, should be expected close to the rod.

It is not unreasonable to expect that the theoretical solution obtained, Eq. 2-2.21, should be compatible with the results for other similar problems.

As a case in point, consider the solution for the flow induced in an annular space, filled with a viscous medium, formed by two concentric infinite cylinders when the inner cylinder (with radius R_1) is given by an axial harmonic oscillation. If the outer radius is R_2, then the differential system may be written (for a parallel flow)

$$\frac{\partial w}{\partial t} = \nu \nabla^2 w \qquad (2\text{-}2.22)$$

with boundary conditions

$$w(R_1, t) = U_o \cos \omega t$$

and

$$w(R_2, t) = 0$$

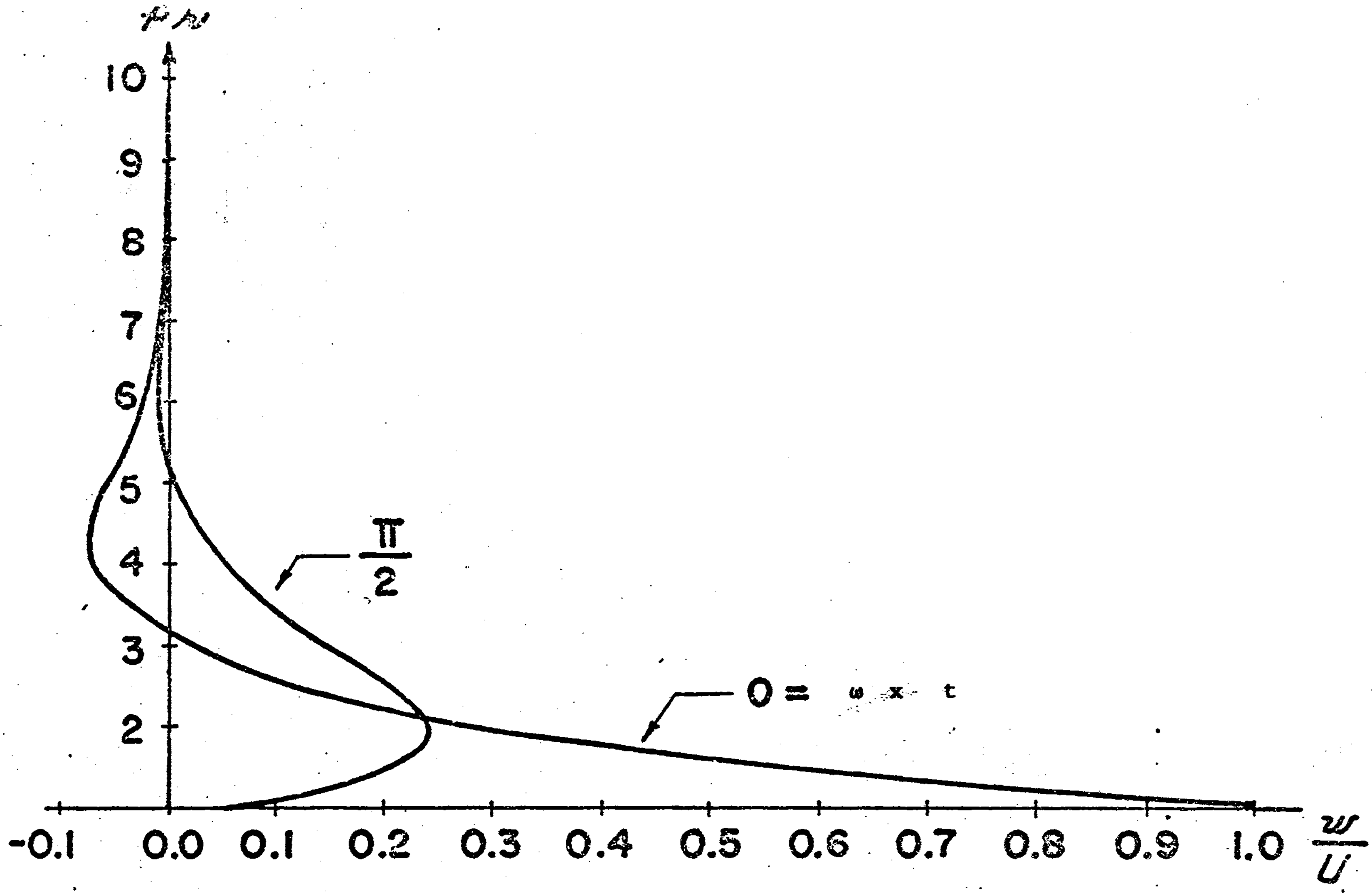

Figure 2. Velocity profile given by Eq. 2-2.21

A solution to the differential equation 2-2.22 is

$$w(R,t) = \left(A\, J_o(i^{3/2}pr) + B\, K_o(i^{1/2}pr)\right) e^{i\omega t} \qquad (2\text{-}2.23)$$

Substituting the boundary conditions, one obtains

$$e^{i\omega t}\left(A\, J_o(i^{3/2}pR_1) + B\, K_o(i^{1/2}pR_1)\right) = U_o \cos \omega t \qquad (2\text{-}2.24)$$

and

$$e^{i\omega t}\left[A\, J_o(i^{3/2}pR_2) + B\, K_o(i^{1/2}pR_2)\right] = 0 \qquad (2\text{-}2.25)$$

If $\eta = i^{3/2}pr$

and $\zeta = i^{1/2}pr$

then

$$A = -B\,\frac{K_o(\zeta_2)}{J_o(\eta_2)} \qquad (2\text{-}2.26)$$

and
$$B\left(K_o(\zeta_1) - \frac{K_o(\zeta_2)\, K_o(\zeta_1)}{J_o(\eta_2)}\right) = U_o$$
$$(2\text{-}2.27)$$
$$B = \left(K_o(\zeta_1) - \frac{K_o(\zeta_2)\, K_o(\zeta_1)}{J_o(\eta_2)}\right)^{-1} U_o$$

As $R \rightarrow \infty$,

and $\zeta_2 \rightarrow \infty$,

$\eta_2 \rightarrow \infty$.

Since

$J_o(\eta_2) \rightarrow 0$

$K_o(\eta_2) \rightarrow 0$

as

$R_2 \rightarrow \infty$,

$A = 0$

$$B = \left(K_o(\zeta_1)\right)^{-1} U_o \qquad (2\text{-}2.28)$$

which then gives a velocity profile

$$w(r,t) = \frac{U_o \cos \omega t}{K_o(\zeta_1)} K_o(\zeta) \tag{2-2.29}$$

This is identical to the solution obtained for the infinite case, as it should be if the two solutions are to be consistent.

Equation 2-2.19 can also be written in a complex form since

$$K_o(i^{1/2}pr) = N_o(pr) \exp(i\phi_o(pr))$$

Then the velocity distribution, Equation 2-2.19, becomes

$$w(r,t) = U_o e^{i\omega t} \frac{N_o(pr)}{N_o(pR)} \exp [i(\phi_o(pr) - \phi_o(pR)] \tag{2-2.30}$$

or

$$w(r,t) = U_o \frac{N_o(pi)}{N_o(pR)} \exp [i(\omega t + \phi_o(pr) - \phi_o(pR))] \tag{2-2.31}$$

McLachlan and Meyers (16) have shown that Eq. 2-2.30, for large values of r, may be written

$$w(r,t) = U_o \left(1 + \frac{y}{R}\right)^{-1/2} [\exp((\frac{-\rho\omega}{2\mu})^{\frac{1}{2}}y)] \cos (\omega t - (\frac{\rho\omega}{2\mu})^{\frac{1}{2}}y) \tag{2-2.32}$$

If the distance from the oscillating rod is designated as y, then

$$w(r,t) = U_o \left(1 + \frac{y}{R}\right)^{-1/2} [\exp((\frac{-\rho\omega}{2\mu})^{\frac{1}{2}}y)] \cos (\omega t - (\frac{\rho\omega}{2\mu})^{\frac{1}{2}}y) \tag{2-2.33}$$

Now as

$$R \to \infty$$

$$w(r,t) \to U_o [\exp(-(\frac{\rho\omega}{2\mu})^{\frac{1}{2}}y) \cos (\omega t - (\frac{\rho\omega}{2\mu})^{\frac{1}{2}}y) \tag{2-2.34}$$

which is the corresponding solution for the oscillating plate problem.

Since the solution obtained for the oscillating infinite rod, Eq. 2-2.21, satisfies the governing differential equation and the initial and boundary conditions, and further is compatible with similar closely related problems, Equation 2-2.21 can be considered to be an acceptable formal solution for the velocity induced by an oscillating infinite rod in a viscous medium of infinite extent.

2-3. Conservation of Mass

The continuity equation must also be satisfied. In cylindrical coordinates this may be written

$$\frac{\partial u}{\partial r} + \frac{u}{r} + \frac{1}{r}\frac{\partial v}{\partial \Theta} + \frac{\partial w}{\partial z} = 0 \tag{2-3.1}$$

Since u and v are assumed identically zero, and $w = w(r,t)$ then

$$\frac{\partial w}{\partial z} = 0$$

so that the solution obtained also satisfies continuity.

2-4. Wall Shear Stress

Since for a Newtonian fluid the shear stress and strain rate are linearly related by the relationship

$$\tau = \mu\frac{\partial w}{\partial r} \tag{2-4.1}$$

the shear stress at the wall, τ_o, may be evaluated by

$$\tau_o = \mu\frac{\partial w}{\partial r}\bigg|_{r = R} \tag{2-4.2}$$

The strain rate, $\frac{\partial w}{\partial r}$, may be obtained by differentiating equation 2-2.21 to obtain

$$\frac{\partial w}{\partial r} = \frac{U_o p}{\ker^2 pR + \mathrm{kei}^2 pR}\left[(\ker' pr \ker pR + \mathrm{kei}' pr\, \mathrm{kei}\, pR)\cos wt - (\mathrm{kei}' pr \ker pR - \ker' pr\, \mathrm{kei}\, pR)\sin wt\right] \tag{2-4.3}$$

hence

$$\left.\frac{\partial w}{\partial r}\right|_{r=R} = \frac{U_o p}{ker^2 pR + kei^2 pR} \left[(ker' \, pR \; ker \, pR + kei' \, pR \; kei \, pR) \cos wt - (kei' \, pR \; ker \, pR - ker' \, pR \; kei \, pR) \sin wt \right] \quad (2\text{-}4.4)$$

Values for the derivatives, $ker' \, pR$ and $kei' \, pR$, for a given value of the argument have been tabulated by Flugge (4).

A dimensionless shear stress may be defined by

$$\tau^* = \frac{1}{U_o p} \left.\frac{\partial w}{\partial r}\right|_{r=R} \qquad (2\text{-}4.5)$$

hence,

$$\tau^* = \frac{1}{ker^2 pR + kei^2 pR} \left[(ker' \, pR \; ker \, pR + kei' \, pR \; kei \, pR) \cos wt - (kei' \, pR \; ker \, pR - ker' \, pR \; kei \, pR) \sin wt \right] \quad (2\text{-}4.6)$$

Figure 3 portrays the variation in the dimensionless shear stress over a half cycle. As should be expected, the shear stress varies harmonically with time.

2-5. Transition to Turbulent Flow

Of prime importance is the question of when the unsteady laminar flow induced by the harmonic oscillation of the rod will break down, resulting in a turbulent flow. It would be most desirable to effect a prediction, from theoretical considerations, of the conditions under which transition will occur. As has been indicated by a number of investigators, including Sarpkaya (21), O'Brien and Logan (18), and Combs and Gilbrech (2), the current state of knowledge of unsteady laminar flow does not allow a theoretical analysis of this problem; hence a theoretical study was not undertaken in this

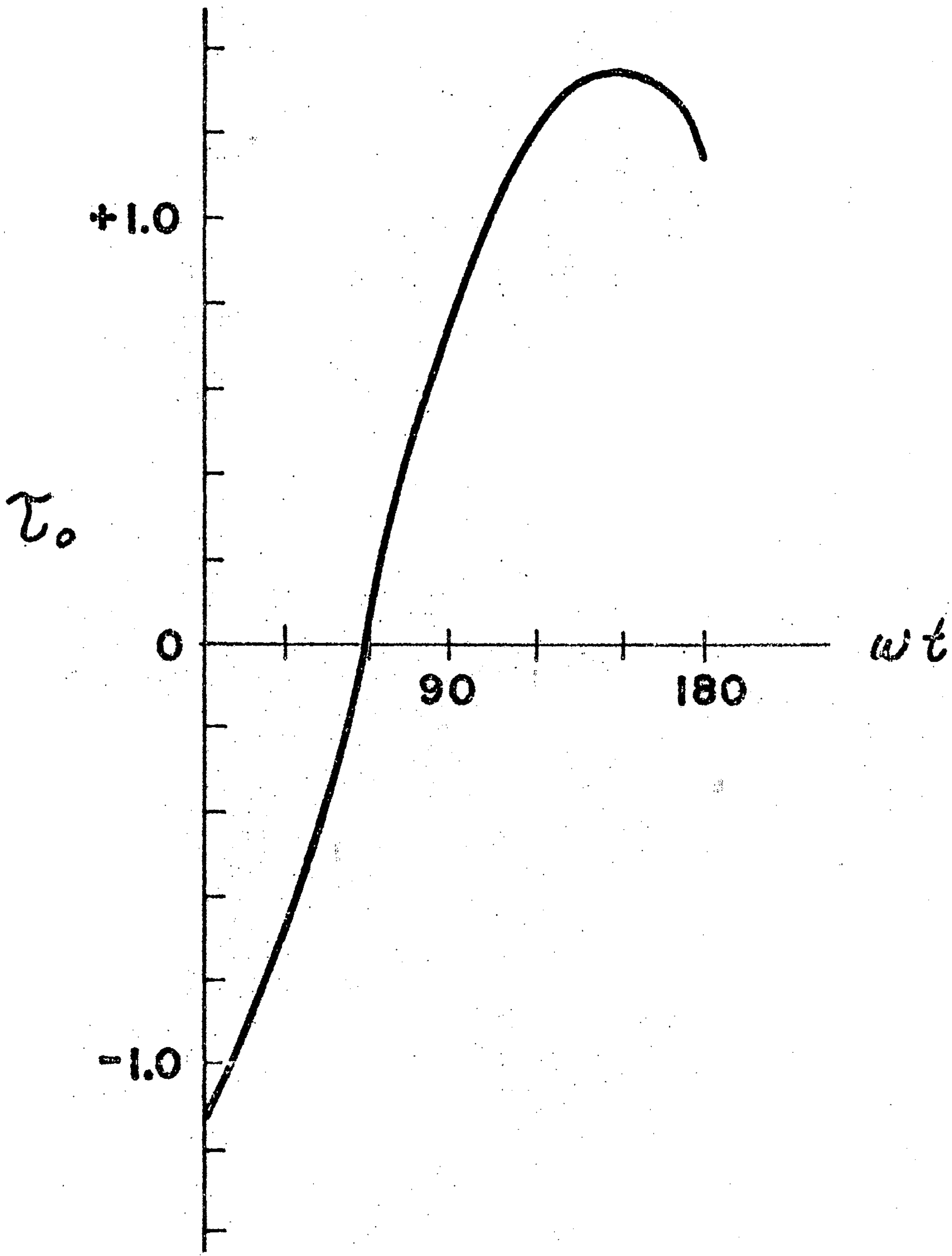

Figure 3. Dimensionless shear stress as given by Eq. 2-4.6.

investigation. Sarpkaya's study (21) of the mechanism of turbulence generation at least provides some insight into this problem in unsteady viscous flow. Based upon phenomenological data, as well as experimental studies of the growth of turbulent plugs, it was determined that

(1) the transition process in an unsteady flow is gradual in onset.

(2) instability in the flow is a consequence of the interaction between double inflection points in the velocity field, flow reversal on the pipe wall, and fluctuation in the shear stress in the flow.

While the problem studied was not identical, nonetheless, the conclusions reached are meaningful in attempting to describe the transition process in an unsteady viscous flow.

CHAPTER III

Experimental Considerations

3-1. Introduction

While the theoretical analysis contained in Chapter II yielded a solution which satisfied

(1) the differential equation,

(2) the boundary conditions,

and which was compatible with solutions for similar problems, the question of its applicability to a real flow still remained unanswered. In view of this, an experimental study was undertaken to obtain actual velocity profiles to verify the correctness and applicability of the theoretical analysis. It is the purpose of this Chapter to describe:

(1) the apparatus utilized,

(2) the instrumentation,

(3) certain preliminary tests, and

(4) the experimental procedure used.

3-2. Apparatus

The apparatus utilized for this study consisted of a rectangular Plexiglas tank, the outside dimensions of which were 24 inches long, 7 inches wide, and 12 inches high. The thickness of each wall was 1/4 inch. Holes were drilled through either end of this tank and small Teflon bearings were positioned so that a long 3/8 inch polished stainless steel rod could be freely oscillated parallel to the 24 inch dimension and the bottom of the tank.

The tank dimensions were selected to allow velocity measurements near the center of the tank, a location which would be free of wall and end effects. Plexiglas was used so that photographic flow visualization studies could be made.

The diameter of the oscillating rod was selected to provide a member capable of carrying its own weight without significant deflection. In addition, the oscillating member was to be stiff enough to preclude buckling under the action of the axial driving force. The 3/8 inch rod selected presented no problems in simulating the boundary conditions associated with the theoretical analysis. A stainless steel rod was selected to facilitate flow visualization studies in dilute polymer solutions. Since this aspect of the investigation was altered during the course of the study, any material would have been equally satisfactory.

In addition to the tank and rod combination, some means of giving the rod the desired motion for a range of oscillation frequencies and amplitudes was required. To accomplish this, the rod was driven by a 3000 rpm universal motor through a ten to one speed reducer and a scotch yoke. The scotch yoke was constructed to provide three different amplitudes. Figure 4 is a plot of a true sine curve as compared with the output motion from the scotch yoke. In view of the small deviation of one curve from the other, it was felt that a good approximation to true harmonic motion was obtained. The electrical input to the motor was through a General Electric electronic speed control which allowed variation of the rate of oscillation from 50 cpm to 300 cpm. A small microswitch was so positioned that when the rod was in one extreme position a circuit would be closed driving an event marker in the recorder used to obtain velocity data. This

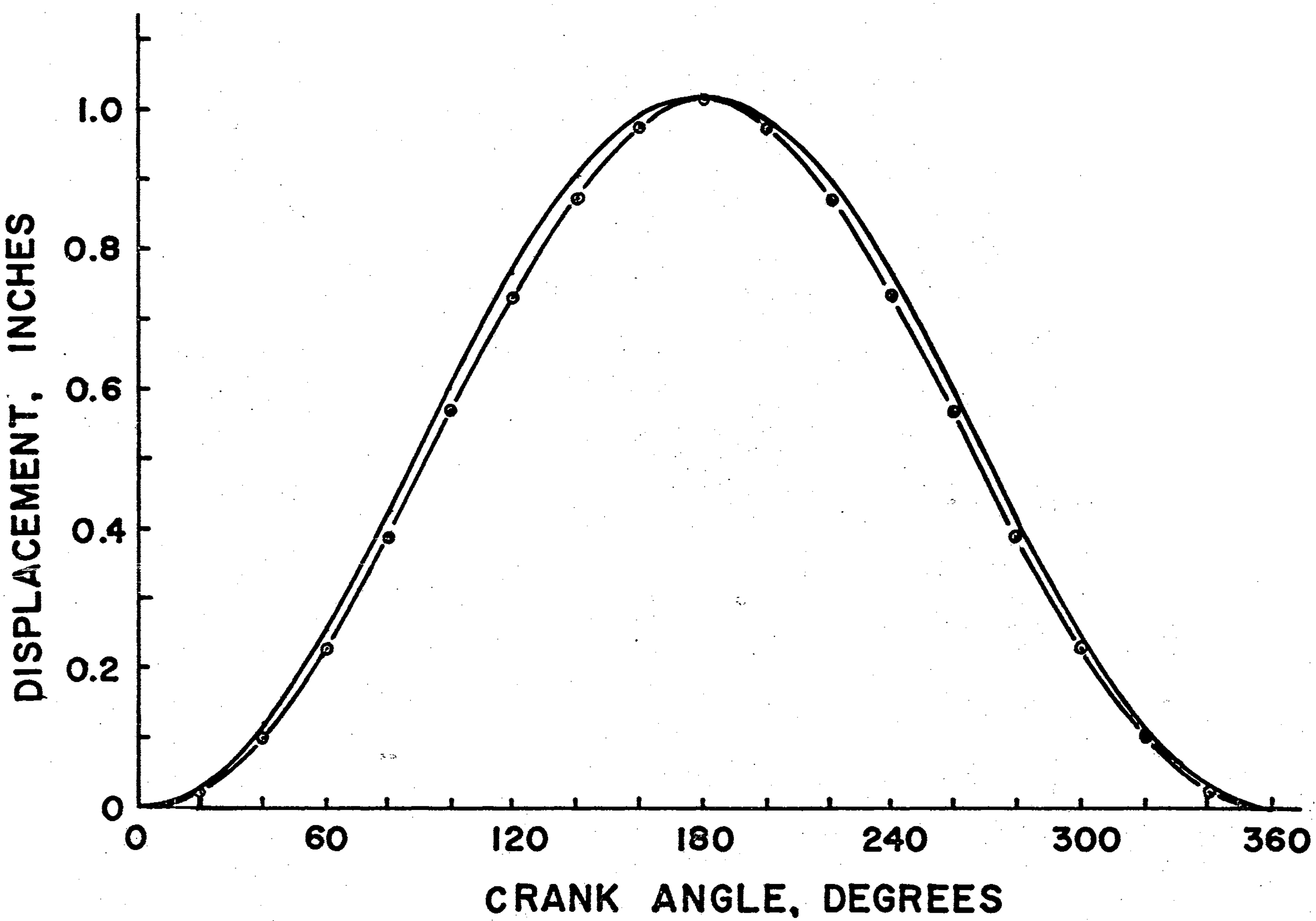

Figure 4. Rod displacement curve

auxiliary system provided the capability for determining phase shifts in the induced velocity profile.

A photograph of the tank and rod assembly is shown in Figure 5.

3-3. Instrumentation

The instrumentation required to obtain the desired velocity data was not extensive and essentially consisted of three distinct systems which were:

(1) Hot wire probe and probe positioning system.

(2) Probe power source.

(3) Data acquisition system.

The hot wire probe was a standard low temperature probe supplied by the Flow Corporation. The wire was tungsten of 0.00035 inch diameter and length 0.044 inches. To position the hot wire, the probe was attached to a rack and pinion with an attached vernier scale which read to 0.1 millimeter. It was found that this experimental technique gave a good representation of the experimental data. The rack and pinion, actually a microscopic focusing unit, gave an accurate, convenient, and positive means of positioning the probe.

The use of hot film equipment in flow measurement is based upon the theory that when a heated wire is placed in a fluid stream, heat transfer from the wire to the fluid will occur. This will, in turn, produce a lower wire temperature, a consequence of which is a change in the electrical resistance of the wire. If a constant current is passed through the wire, the variation in the electrical resistance will give rise to a variation in the voltage drop across the wire. By suitable calibration this voltage drop can be made to indicate the velocity of the fluid passing over the wire.

In practice the hot wire sensor is usually used as one leg of a

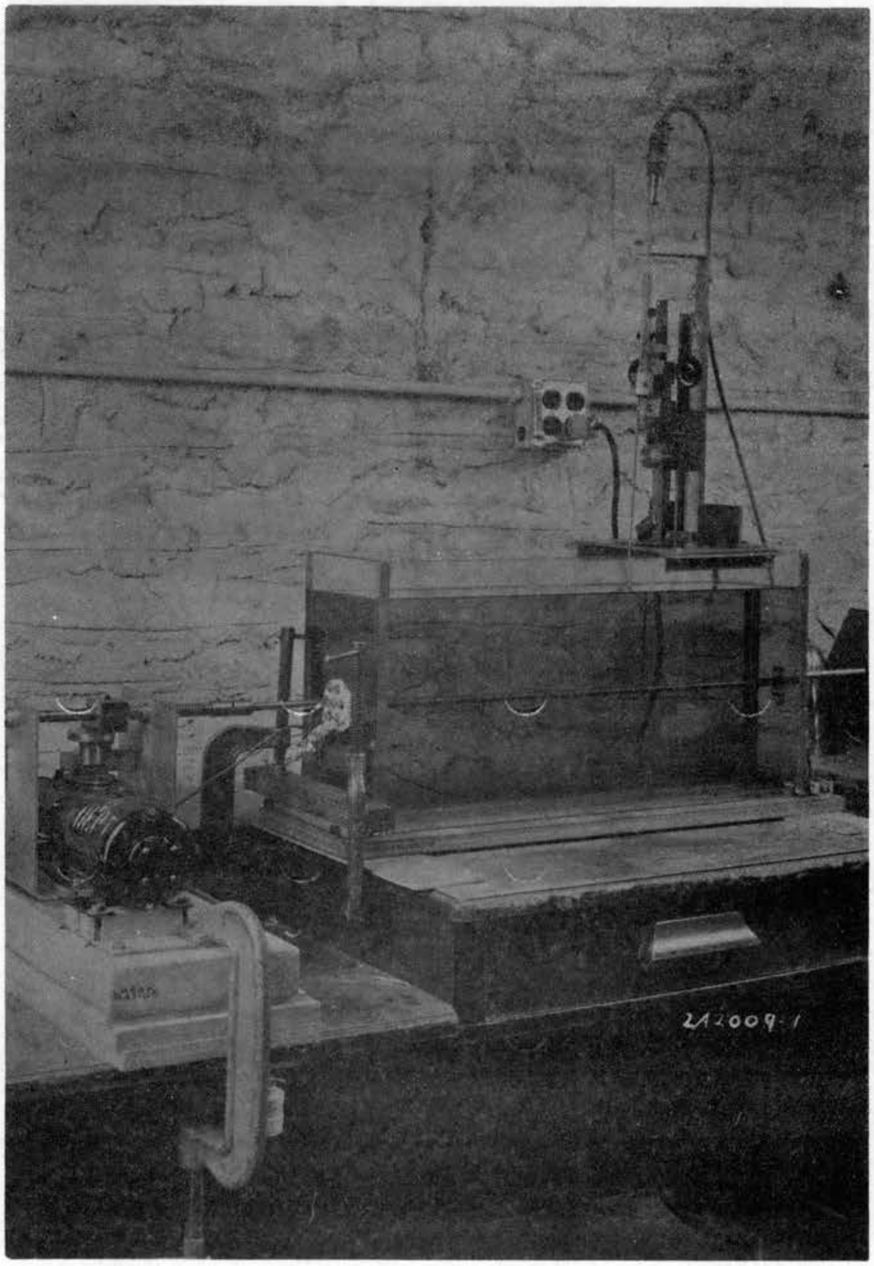

Figure 5. Experimental apparatus

SCHEMATIC DIAGRAM OF DATA ACQUISITION SYSTEM

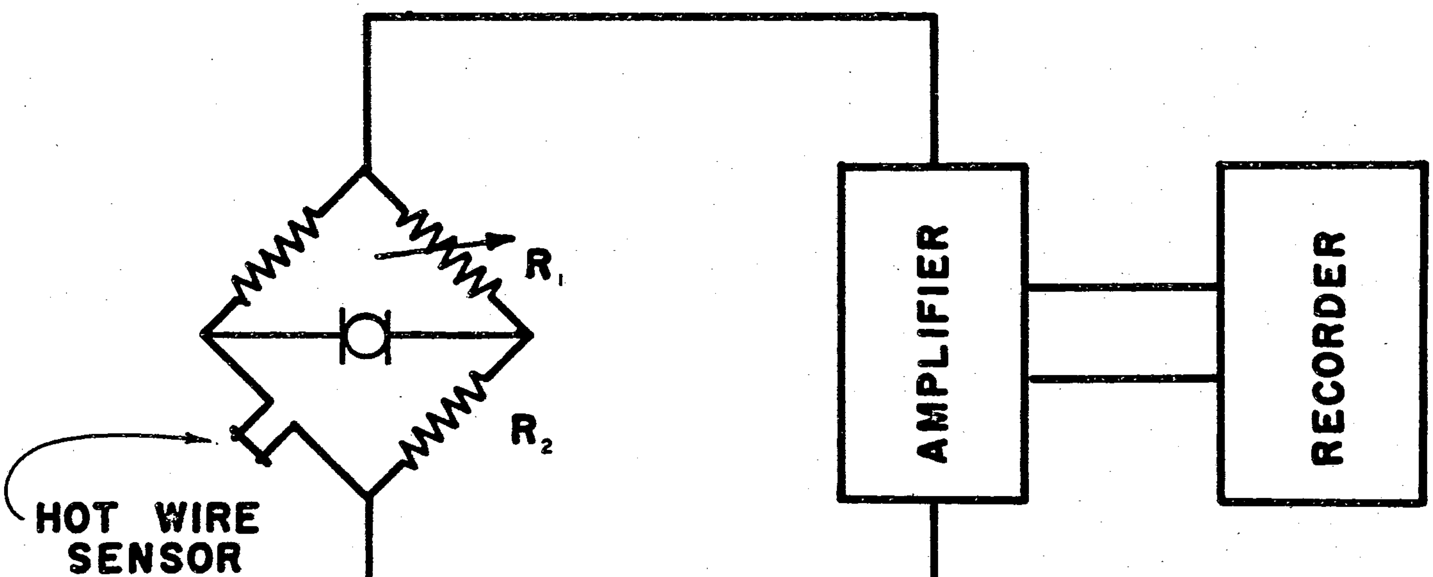

Figure 6. Data acquisition system

resistance bridge, as shown in Figure 6, and the output voltage from the bridge is taken as an indication of the fluid velocity over the sensor. In the studies described herein, this procedure was followed.

To achieve constant current through the sensor, a large resistor was placed in series with the sensor so that the small variations in sensor resistance had a negligible effect upon the wire current. Referring to Figure 6 , the sensor resistance (cold) was 1.0 ohms and the series resistor, R_2, was 390 ohms. For an impressed voltage, E, of ten volts, the wire current was slightly greater than 25 milliamperes.

The choice of magnitude of the wire current was a compromise. The higher the wire current, the more sensitive the anemometer and likewise, the greater the power dissipation from the wire. Initial studies with a wire current of one hundred fifty milliamperes demonstrated a well-defined free convection field about the sensor. Since this was deemed undesirable, because of the possible effect of the fluid velocity induced by the free convection from the wire, the current level was reduced sharply. It was found that a wire current of 25 milliamps was quite ample, with no apparent convection field, but that the output voltage required amplification in order to drive the strip chart recorder. For this reason the signal from the hot wire was amplified by a Nanovolt direct current amplifier, with a gain of 1000, before it was sent to a Brush Mark II recorder. The resulting output then was a time-voltage strip chart which could then be translated into the velocity time variation at a given point in the flow. Because the hot wire sensor was positioned as close as 0.1 millimeter to the moving surface, wall effects upon heat transfer from the sensor were considered. Grant and Kronauer (7) have indicated that:

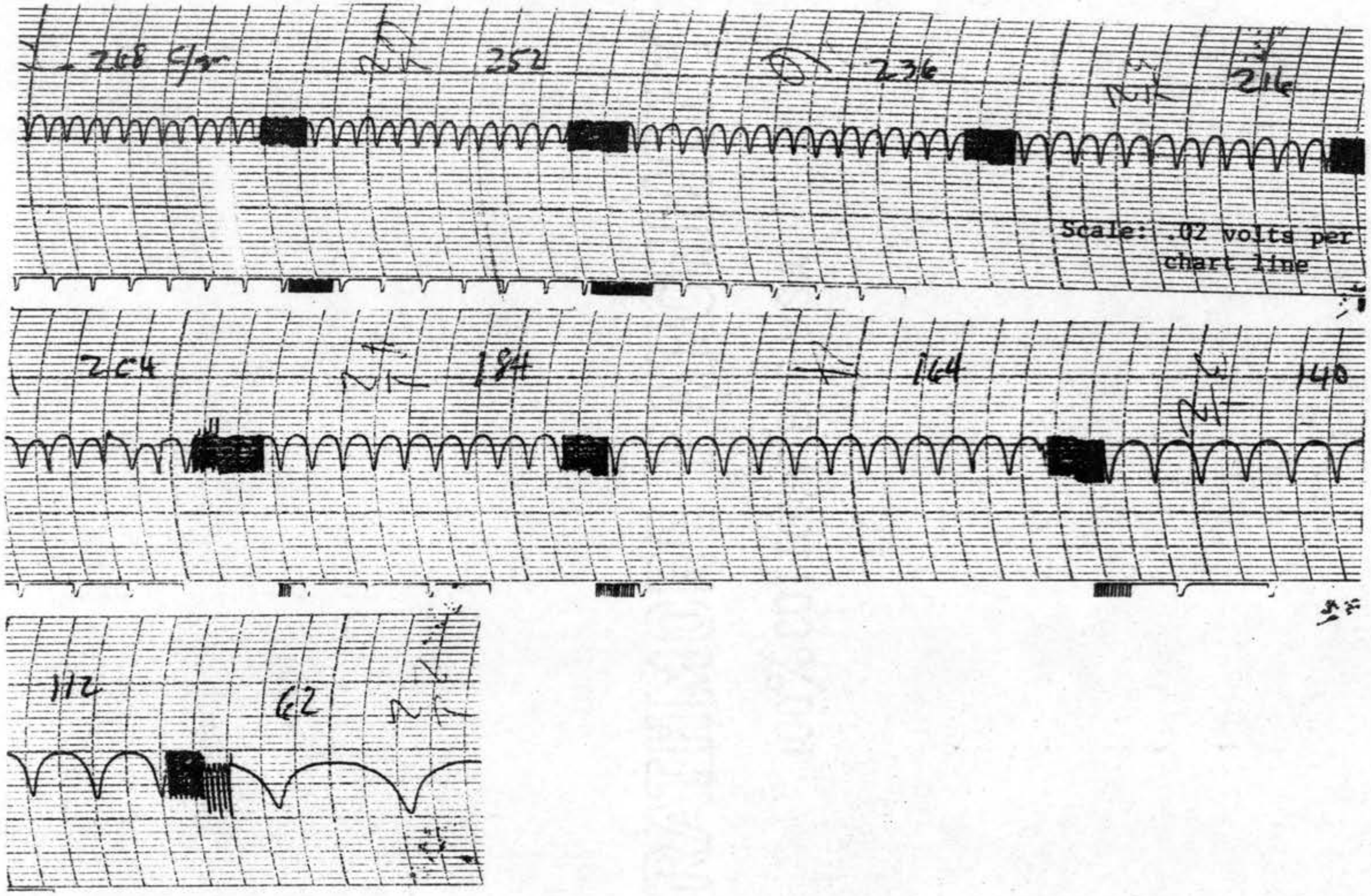

Figure 7. Typical calibration data

(1) radiation effects may be neglected when compared with convective effect.

(2) Convective effects will be of consequence when the sensor is closer to the surface than $\frac{D}{N_N}$, and that a distance $\frac{5D}{N_N}$ may be considered as "remote".

Based upon the analysis in Appendix B, a reasonable value for the quantity $\frac{5D}{N_N}$ was 0.00076 inches, while the shortest distance from the oscillating rod to the sensor was 0.00394 inches. Wall effects were neglected as a consequence of this analysis.

3-4. Sensor Calibration

To interpret the velocity data acquired, it was necessary to calibrate the anemometer output. To accomplish this, the sensor was placed as closely as possible to the oscillating surface. The rod was then driven at several different rates of oscillation, while the oscillation amplitude was held constant. A typical resulting strip chart is shown in Figure 7. Note that the fluid this close to the oscillating surface was moving in phase with the rod motion since the points of flow reversal (the low points on the strip chart) corresponded to the extreme points of the rod motion, as indicated by the pips on the event marker. In view of this, the peak on the strip chart was associated with the maximum rod velocity, the product of amplitude and frequency. By noting the pen deflection of the recorder corresponding to this peak velocity, a calibration curve, Figure 8 was developed. Figure 8 reflects calibration data for a rod oscillation of 268 cycles per minute with an amplitude of one half inch.

3-5. Preliminary Investigations

A number of preliminary studies were carried out in the course

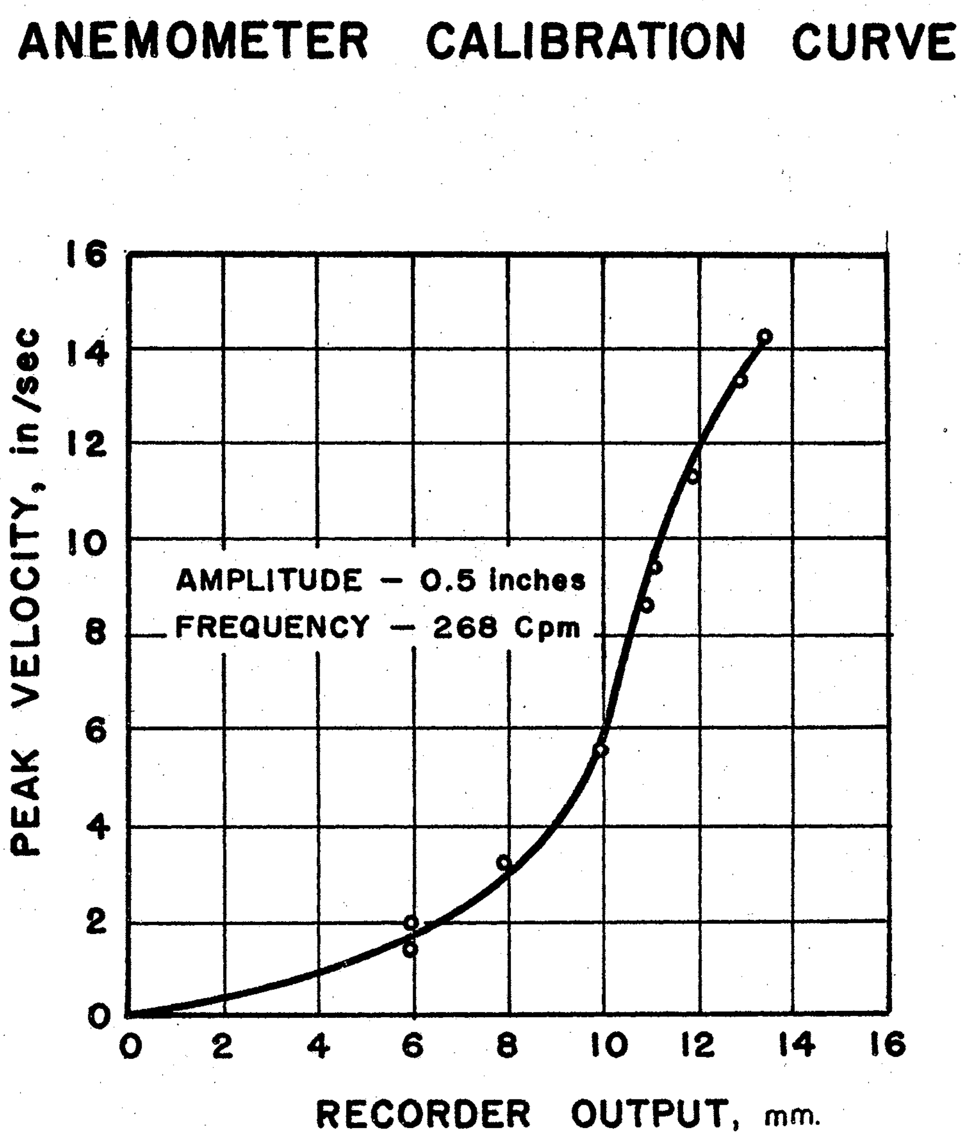

Figure 8. Anemometer calibration curve.

of this investigation. It is hoped that the following remarks will give insight into the nature of, as well as indicating the necessity for, these preliminary studies.

Two physical properties, dynamic viscosity and specific gravity, were evaluated at various temperatures for the working fluid. Specific gravity was determined with a hydrometer. Absolute viscosities for the oil were determined with a falling sphere viscosimeter manufactured by Roger Gilmont Instruments, Inc. The viscosimeter was calibrated with a 100 centipoise standard fluid supplied by the Brookfield Corporation; then the calibration was verified by measuring the viscosity of distilled water. Gilmont and Mauser (5) have shown that a suitable equation for the falling sphere viscosimeter as

$$\mu = K(\rho_f - \rho)\ t$$

where K was found (from the calibration studies) to be 2.97 ft^2/sec^2. Physical properties for the oil are shown in Figures 9 and 10.

To insure that the flow remained laminar for the frequencies and amplitudes to be studied, a preliminary study was run with a mixture of Polyor (polyethylene oxide) in distilled water. Because of the streaming birefrigence characteristic claimed by the manufacturer, it was hoped that a breakdown of the laminar flow could be visualized. The solution used contained about 4% Poylox by weight and had a viscosity, at a low strain rate, about four times that of water (as contrasted to a viscosity ratio of about fifty for SAE 10 oil). Because nothing could be seen using polarized light and the Polyox solution, the study was conducted with a dye trace (potassium permanganate) in the Polyox solution. No evidence of turbulent diffusion of the dye trace was observed even at high frequencies immediately after the introduction of the dye, nor after continued oscillation for 3 minutes.

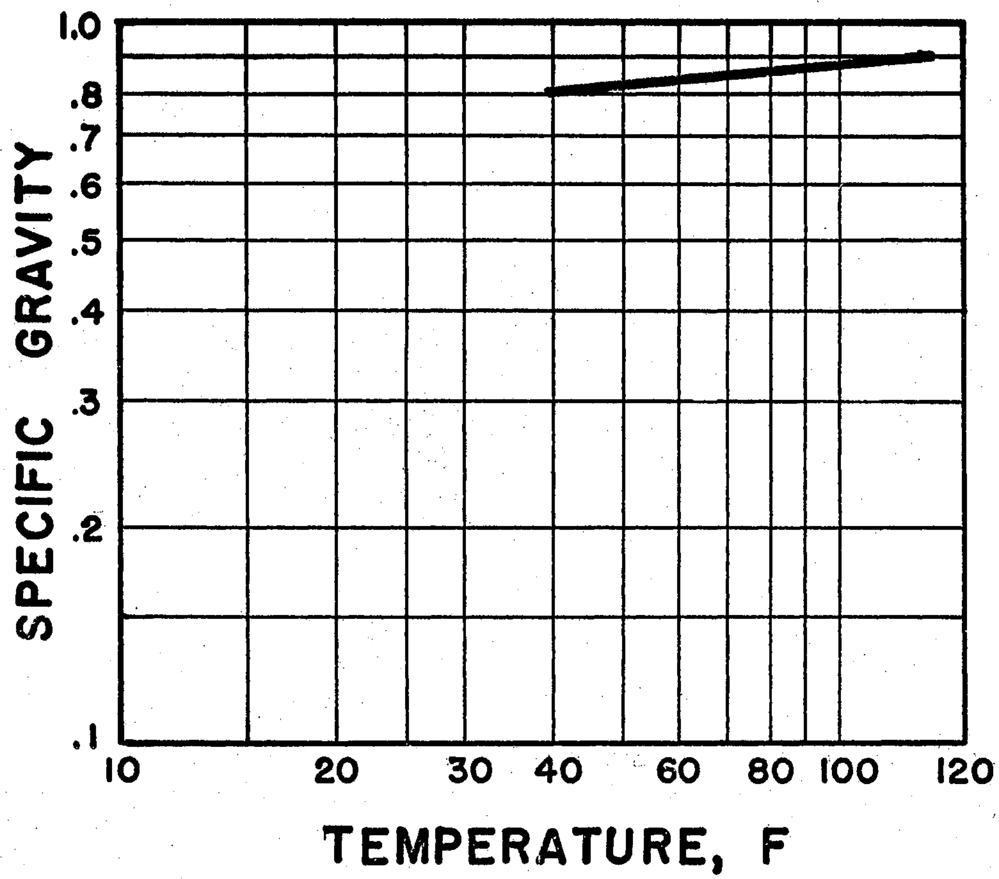

Figure 9. SAE 10 oil specific gravity

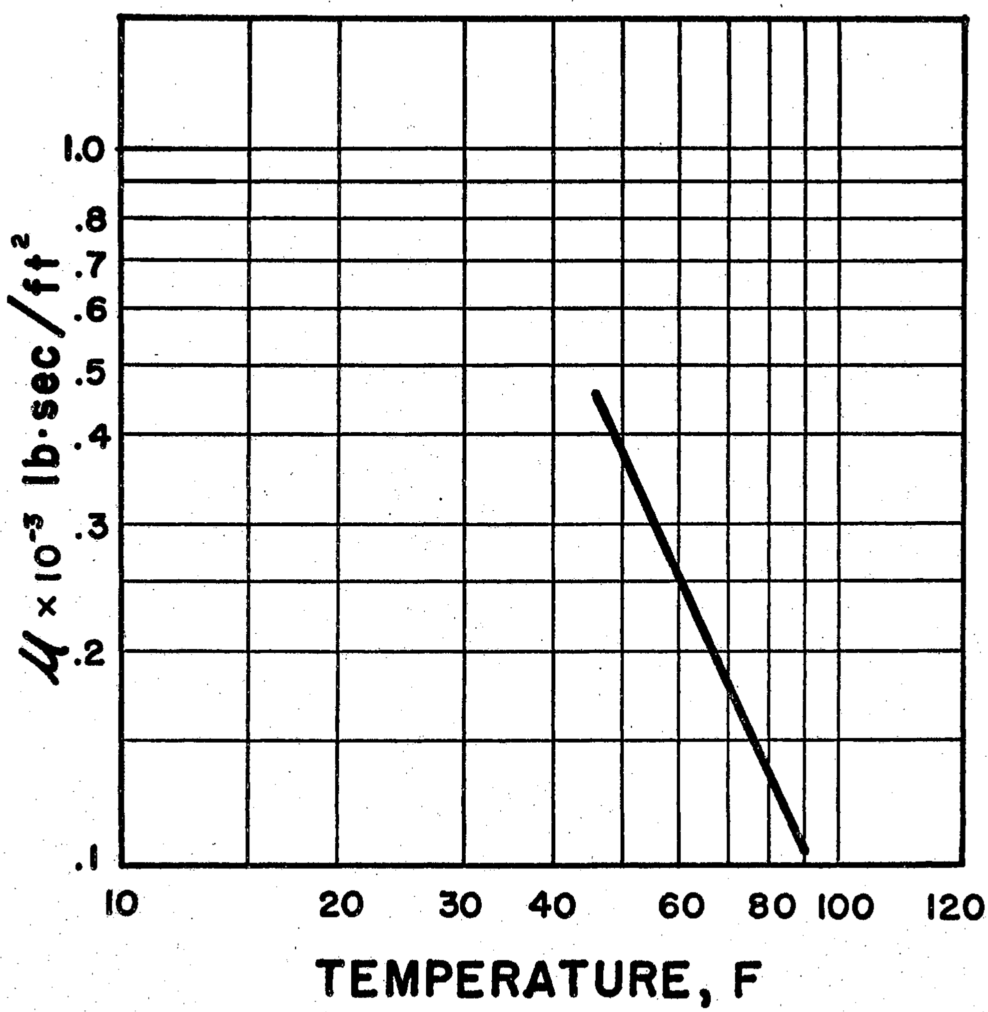

Figure 10. SAE 10 oil absolute viscosity

In addition, no significant translation of the dye trace was observed, which tended to indicate that no significant secondary streaming was induced in the flow, nor was the flow a composite pulsating and oscillating flow as O'Brien and Logan (18) studied. Figure 11 is typical of that which was observed during these tests. The photograph shown, for a frequency of 130 cpm and an amplitude of 0.51 inches, was obtained with a Speed Graphic and high contrast orthochromatic film. Exposure times were about 1/10 second. Similar photographs were obtained at 30 cycles/minute and at 100 cycles/minute.

3-6. Experimental Procedure

The experimental procedure indicated below was identical in each test made during this investigation.

1. Instrumentation power was turned on and the entire data acquisition system was allowed to stabilize for a period of thirty minutes to minimize instrumentation drift due to component temperature changes. Since all of the instrumentation contained only solid state components, except for the recorder, this was required only to prevent recorder drift.

2. Rod oscillation frequently was determined by counting, with a mechanical counter driven by the scotch yoke, for a period of a minute.

3. With rod and fluid at rest and the desired wire current passing through the hot wire probe, the bridge circuit associated with the data acquisition system was balanced. At the same time the hot wire probe was placed as close as possible to the surface of the rod.

4. The rod was then allowed to oscillate at the determined rate and amplitude (fixed by scotch yoke setting), and the recorder was activated to obtain a time-voltage plot from the hot wire probe. Oscillation was stopped and recorder was allowed to return to zero

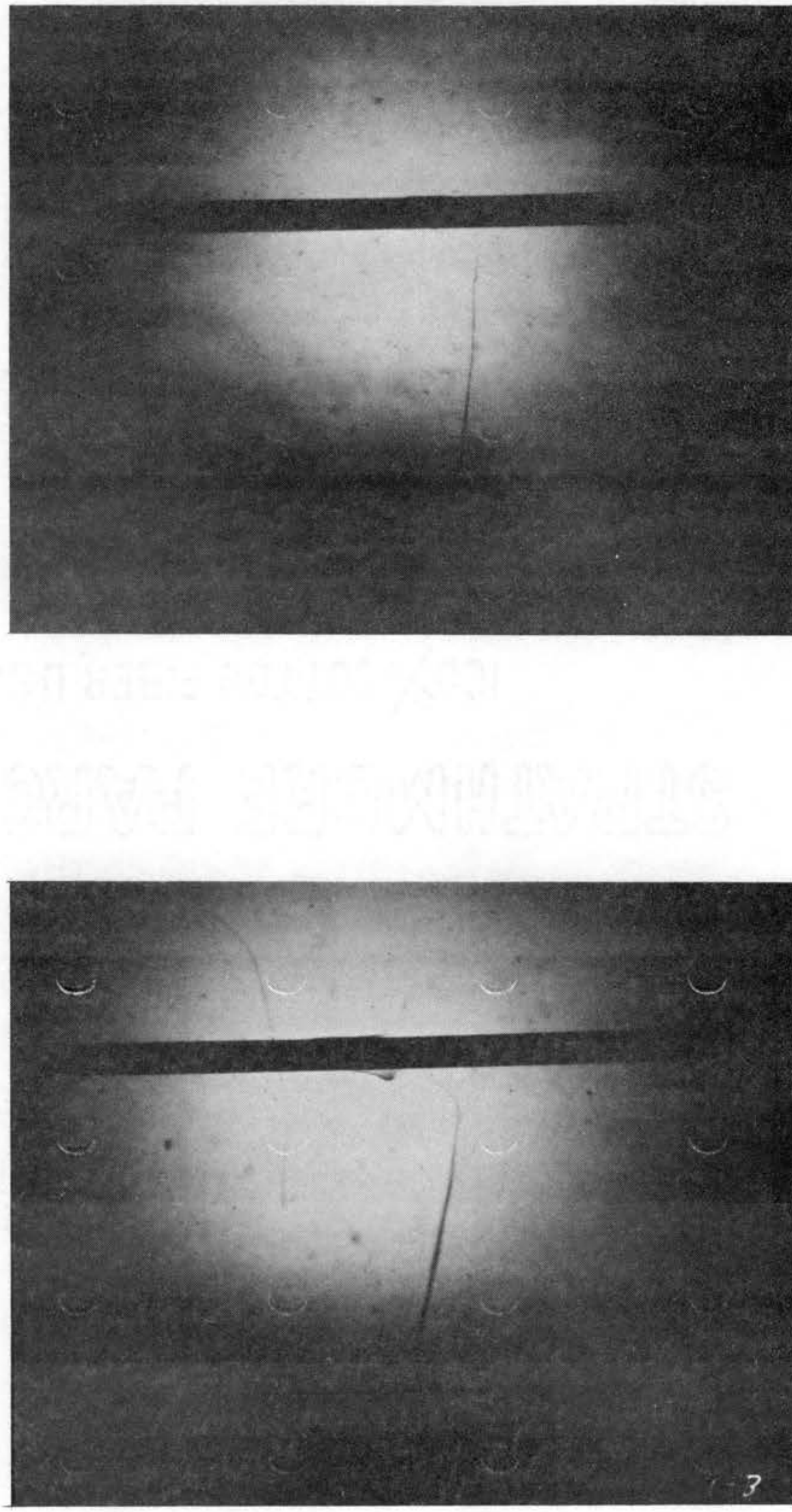

Figure 11. Flow visualization studies

to verify the zero reading.

5. The hot wire probe was repositioned one millimeter from the oscillating rod, and the recording process was repeated. This process was continued, in one millimeter steps, until no wire voltage-time variation could be recorded.

CHAPTER IV

Experimental Results

4-1. Introduction

Using the procedure outlined in the preceding chapter, velocity data were generated for the following rod oscillation conditions:

(1) 62 cpm, 1/4 inch amplitude.

(2) 78 cpm, 3/4 inch amplitude.

(3) 268 cpm, 1/4 inch amplitude.

(4) 268 cpm, 1/2 inch amplitude.

It was intended that experimental verification of the theoretical induced velocity profile would be obtained for three positions in the rod cycle over the experimental range above. In general, good representation of the profile would be most desirable for rod positions of high rod velocity, or for regions of great curvature of the velocity profile, since it is in these positions that transition to turbulence or significant variation in heat or mass transfer coefficients might occur as a consequence of the oscillatory motion. For this reason the rod cycle points selected were:

(1) point of maximum rod velocity.

(2) point one-half way between zero rod velocity and maximum rod velocity.

(3) point of zero rod velocity.

In addition, data were developed to confirm the independence of the induced profile and oscillation amplitude, at a given oscillation rate, as indicated by the theoretical analysis.

Finally, since this experimental study did not produce the transition to turbulence in the induced flow, other similar experimental studies have been reviewed to provide an estimate of the upper limit, in terms of a Reynolds number, for which laminar flow could be expected.

4-2. Experimental Data

Figure 12 is typical of the raw data, in the form of a voltage-time strip chart, which was obtained with the hot wire anemometer. With the aid of sensor calibration data, as well as careful consideration of the strip chart itself, these raw data could be made to yield meaningful velocity data.

Before a detailed discussion of the techniques employed in the reduction of this raw data is made, a few remarks regarding the strip chart itself seem indicated. Of particular interest was the fact that a point representing a zero fluid velocity (point A in Figure 10 for example) does not lie on the zero reference line, which was established for a balanced bridge circuit with the rod at rest. A possible interpretation would be that there existed a translatory secondary flow upon which the oscillatory flow was superimposed. Since the flow visualization study did not indicate the existence of a translatory motion, this possibility was discarded. It seems more likely that this effect was a consequence of a change in sensor resistance which was produced by an increased rate of heat transfer from the sensor, and hence a different sensor temperature, when the fluid was in motion. This explanation was further substantiated by virtue of the fact that as the fluid velocity approached zero, as it did at points in the flow well removed from the oscillating rod, the original zero reference was obtained. While this offered no difficulty in data analysis, it was

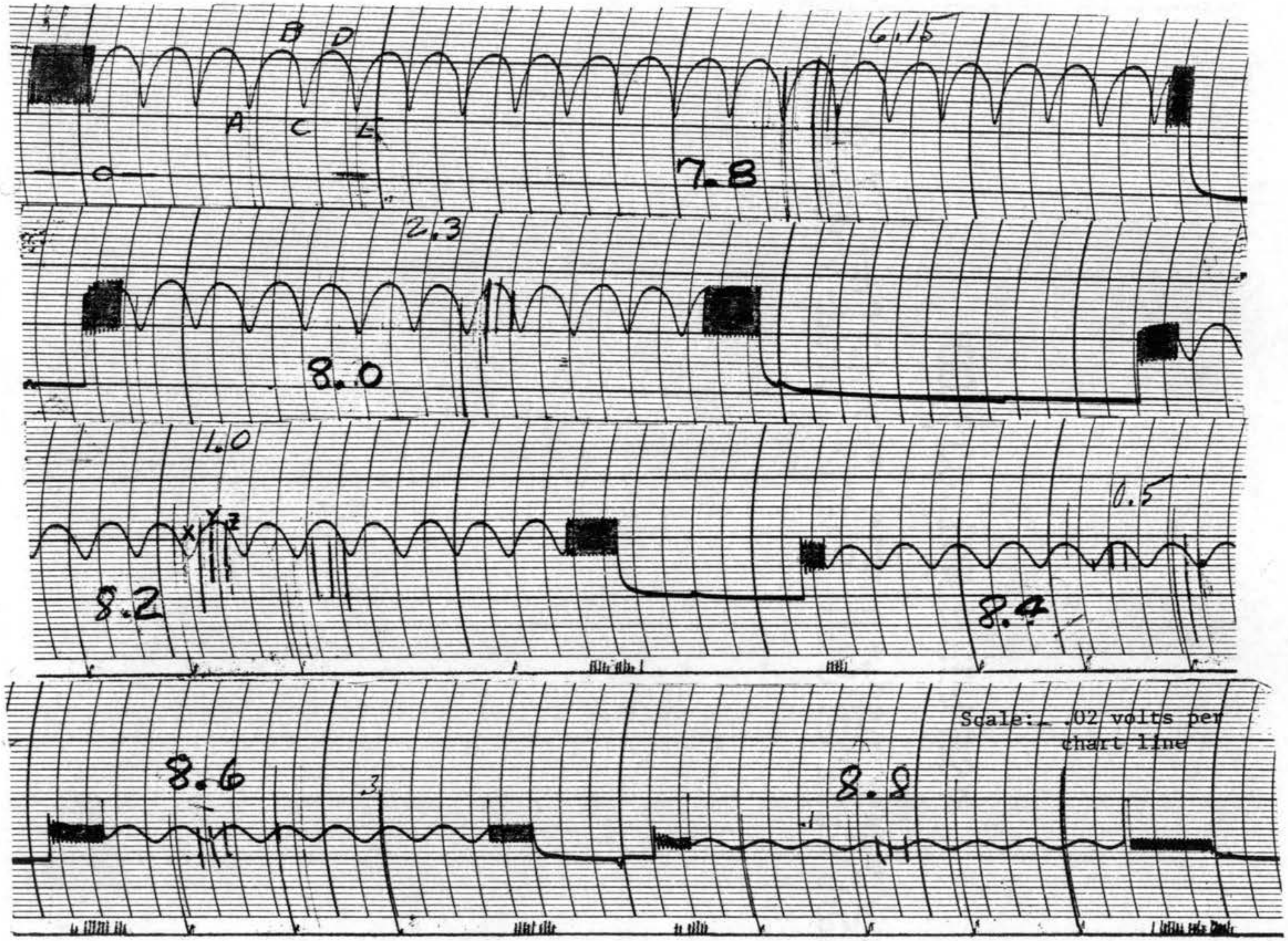

Figure 12. Typical velocity data

felt an attempt to explain this behavior was worthwhile.

An additional bit of useful information was also available from the general appearance of the strip chart. As noted above, the zero velocity reference point established at the beginning of the experimental procedure was again produced when the sensor was located at a point in the flow where the induced fluid velocity approached zero. It was felt that this constituted a satisfactory means of demonstrating that no significant instrument drift had occurred during the experimental procedure.

The desired result from reduction of the experimental data was a determination of the velocity distribution induced in the viscous medium at specified points in the rod cycle. Arbitrarily, the quarter point (termed 0°), three-eights point (termed 45°), and the half point (90°), were selected and velocity data and phasing were developed as indicated in the following sections.

4-3. Phasing

Identification of particular points in the rod cycle was accomplished with the aid of the externally triggered event marker, which was energized, and hence produced a marker pip, at the beginning of each rod cycle. By dividing the total distance between successive pips into eight equal parts, the eighth point and the quarter point in the rod cycle were easily identified. The velocity phase shift which was to be expected as the sensor was moved away from the oscillating surface was quite apparent on the strip chart, Figure 10. When the sensor was positioned close to the oscillating rod (cycle ABC) the induced velocity was in phase with the rod, as it should have been.

4-4. Velocity Determination

Referring to Figure 12 it was noted that with the sensor close to the oscillating surface, point A corresponded to an extreme rod position, and hence a point of zero fluid velocity, while the point B occurred a quarter cycle later and was a point of maximum velocity, since the motion given the rod was harmonic. From the sensor calibration data this peak velocity, at B, was 6.15 inches per second. It was also noted that the difference in pen deflection between A and B was ten scale divisions. To find the velocity at any point along the curve AB, the difference in pen deflection between the unknown point and point A was divided by the difference in pen deflection between A and B, ten divisions. This ratio, termed a scale factor for the lack of a more suitable phrase, was then multiplied by the peak velocity to yield the velocity desired. Finally, this velocity was divided by the maximum rod velocity to yield a dimensionless velocity, which was designated the velocity ratio. This process was repeated with the data acquired at each radial position where at the sensor was located.

4-5. Typical Calculations

Referring to Figure 12 consider the cycle indicated XYZ, which was produced when the rod executed a harmonic motion at a rate of 78 cycles per minute with an amplitude of 0.75 inches. The sensor was located 4 millimeters from the oscillating surface. Then the scale factors were:

(a) 0° 3/6 (c) 90° 6/6

(b) 45° 6/6

The minus sign was used when the eighth point and the quarter point were found on different sides of a zero point in the cycle, the implication being that flow was in the opposite direction, although the directional characteristics could not be determined with the anemometer which was used.

From velocity calibration data:

Peak velocity = 1.0 inch/sec

hence

$$V_X = \frac{3}{6}(1) = 0.5 \text{ inch/sec}$$

$$V_Y = \frac{6}{6}(1) = 1.0 \text{ inch/sec}$$

$$V_Z = \frac{6}{6}(1) = 1.0 \text{ inch/sec}$$

The velocity ratios were:

$$0° \quad : \quad VR = \frac{.5}{6.15} = 0.08$$

$$45° \quad : \quad VR = \frac{1.0}{6.15} = 0.16$$

$$90° \quad : \quad VR = \frac{1.0}{6.15} = 0.16$$

4-6. Tabulated Results

In the manner described above, experimental velocity data were developed for the following rod oscillation conditions.

(1) 62 cycles/min., 1/4 inch amplitude.

(2) 78 cycles/min., 3/4 inch amplitude.

(3) 268 cycles/min., 1/4 inch amplitude.

(4) 268 cycles/min., 1/2 inch amplitude.

The results of these experimental studies are contained in Table I through Table XIII of Appendix C.

4-7. Shear Stress

The theoretical analysis contained in Chapter II included an expression for the wall shear stress. Accordingly, it would be expected that verification of this would be obtained experimentally. A distinct and separate study of this aspect of the problem was not undertaken. However, since inherent in the development of the differential equations of motion is Stokes' Hypothesis, if experimental verification of the induced velocity profile was obtained, then this also provides verification of the expression for shear stress. In view of this, no experimental study, as such, was accomplished.

4-8. Transition

Consideration of the flow visualization study described in Chapter III rapidly led to the conclusion that with the amplitudes and oscillation rates which were available with the test apparatus, transition would not occur for flow induced with a smooth rod. Further confirmation of this came from the studies made by Li (14) wherein, to produce transition of the flow induced by an oscillating smooth plate in water, oscillation amplitudes of 2 to 4 feet and oscillation frequencies of 7 to 16 cycles per minute were required. O'Brien (18), even with a 0.1875 inch half-round disturbance bar on a flat plate was unable to produce transition of the induced flow, when a light paraffin oil was used as the viscous medium, for oscillation rates of 8.4 cycles per second, and oscillation amplitudes of 0.5 inches. Since transition could not be achieved experimentally, the existing literature was reviewed with the express purpose of arriving at some suitable criterion for predicting transition and the onset of turbulence.

Both Combs and Gilbrech (2) and Sarpkaya (22) have studied experimentally pulsating flows in circular ducts. These studies have shown that:

(1) the pulsating pipe flow is more stable than the corresponding steady pipe flow.

(2) the critical Reynolds number, under the simplest conditions must depend upon pulsation frequency as well as the amplitude of the pulsation.

As has been pointed out earlier, the only experimental study wherein an induced flow did undergo transition is the work of Li (14), who studied the flow induced in a large body of water by the harmonic oscillation of a flat plate. His studies indicated that, for a smooth plate, transition occurred for a critical Reynolds number,

$$N_R = \frac{\omega^{1/2} d_1}{\nu^{1/2}} = 800 ,$$

where d_1 is the total displacement of the plate during a half cycle.

In view of the similarity that exists between rod-induced profiles and plate-induced profiles, it was felt that a reasonable estimate of the critical Reynolds number was, $N_R = 800$. At the same time it was recognized that additional research into transition effects should be undertaken to obtain a more accurate transition Reynolds number for the oscillating cylinder.

The maximum Reynolds number for the experimental portion of this study was 0.897.

CHAPTER V

Closure

5-1. Comparison of Experimental and Theoretical Results

Figures 13, 14, 15, and 16 show the theoretical solution, as given by equation 2-2.21, as a solid curve, while the results of the experimental studies are indicated as points thereon. Study of these figures indicates that the data scatter badly for the 62 cpm oscillation rate, but the scatter decreases as the oscillation rate increases. Experimental data for the 78 cpm and the 268 cpm oscillation rates show good agreement with the corresponding theoretical solution.

Sources of error in the experimental study have been considered in Appendix B. This review of possible sources of experimental error indicates that the inability of the anemometer to sense low fluid velocities during the calibration procedure as well as during the actual tests could have been a primary source of experimental error in this study. The data scatter indicated above was probably a consequence of this low anemometer sensitivity, since better results were obtained, in general, as the rod velocity was increased.

Comparison of Figures 15 and 16 will confirm, as the theoretical study indicated, that for a fixed oscillation rate, the induced velocity profile is independent of the oscillation amplitude.

The question of application of the theoretical results to a finite body of viscous fluid requires careful consideration. Certainly the experimental study was done in a container of finite

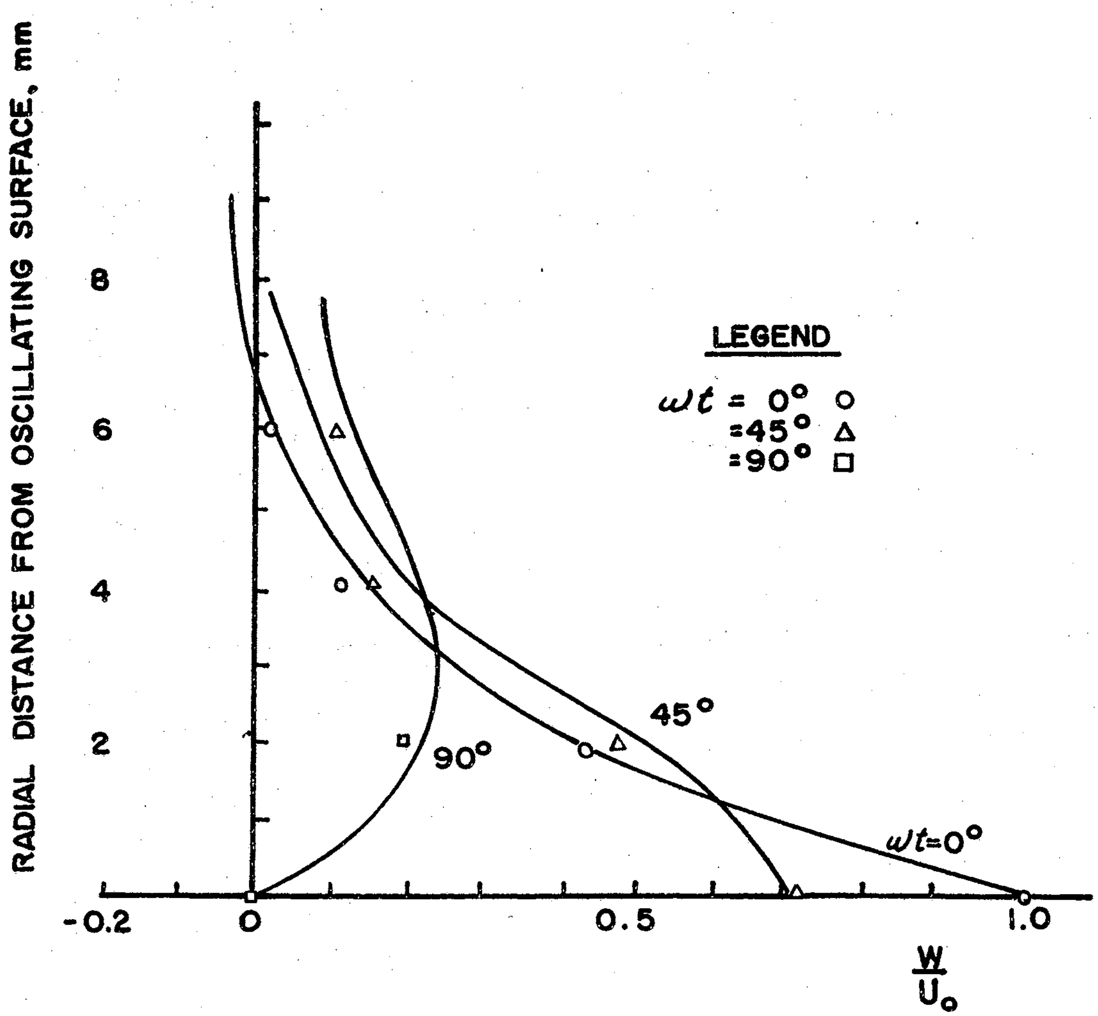

Figure 13. Experimental results, 62 cpm

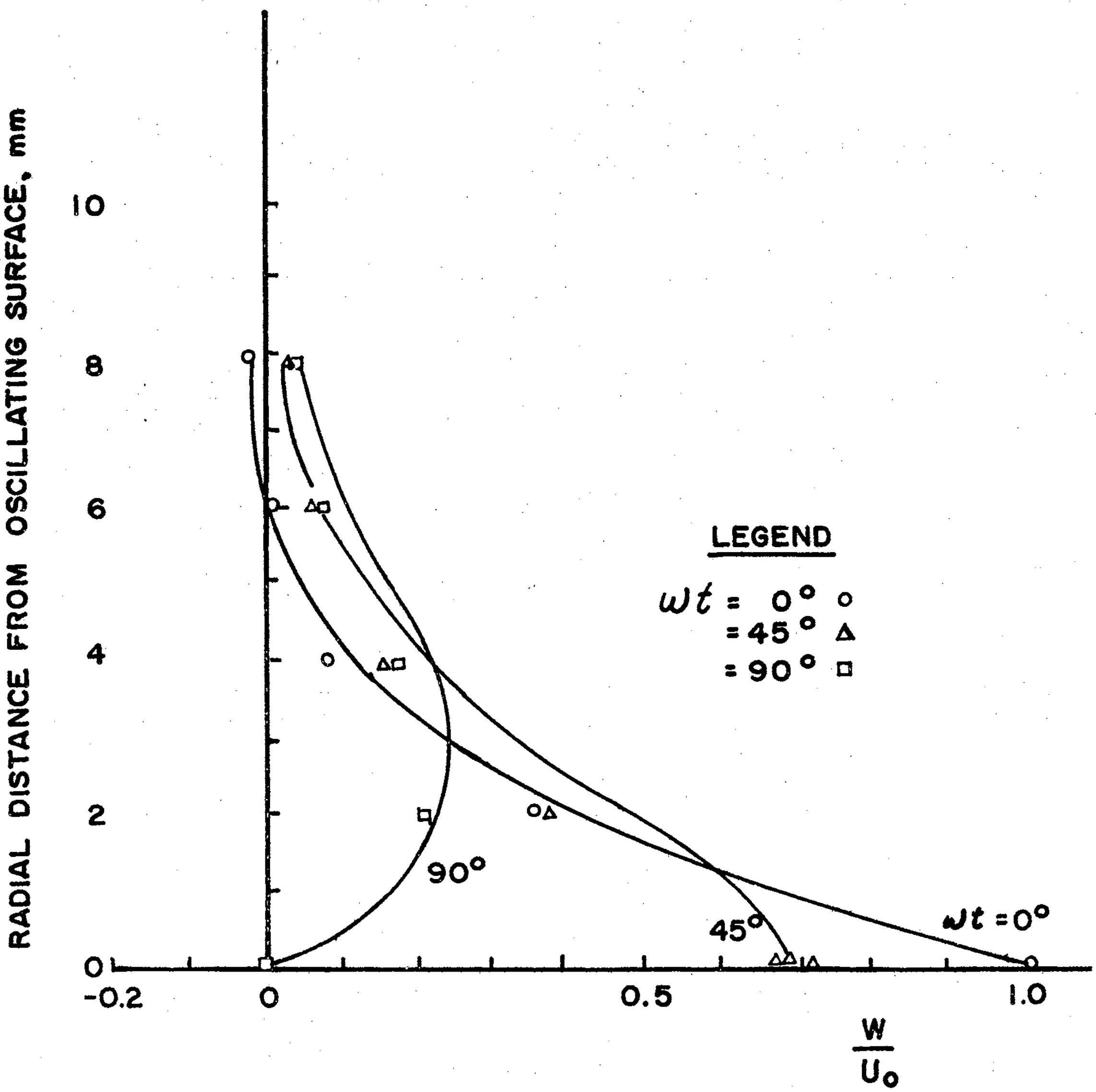

Figure 14. Experimental results, 78 cpm

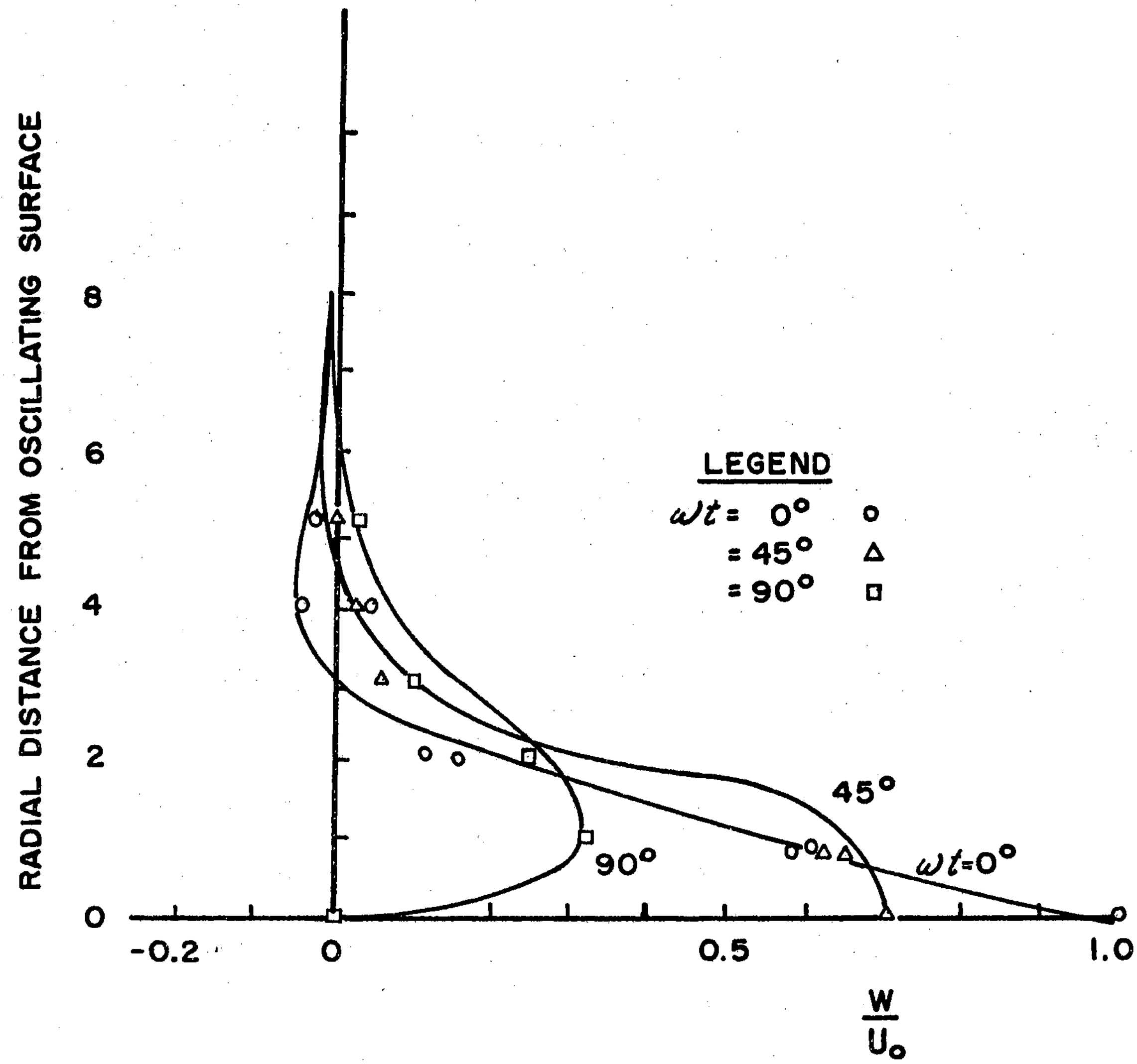

Figure 15. Experimental results, 268 cpm, 1/4 inch

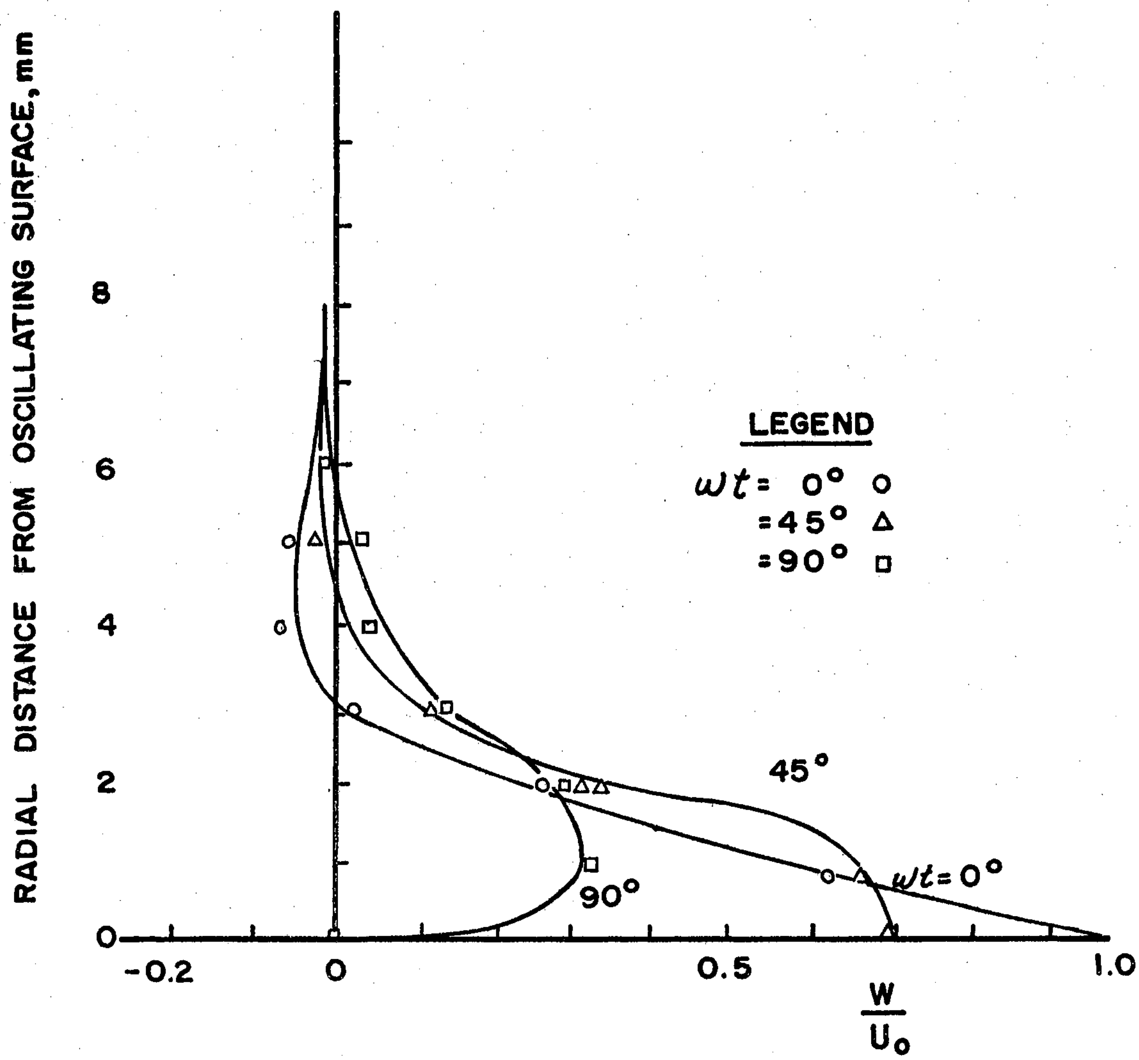

Figure 16. Experimental results, 268 cpm, 1/2 inch

extent, and experimental confirmation of the theoretical analysis was obtained at a point in the fluid which was:

(1) well removed from either end of the tank.

(2) well removed from either side of the tank.

In this light, the fluid in which the sensor was placed was not aware of the end and wall constraint, hence it responded as if the body of fluid was infinite. Figure 2 indicates that the induced velocity should approach zero (actually a velocity too low to be detected) for value of

$$Y_o \left[\frac{\rho\omega}{\mu}\right]^{\frac{1}{2}} = \eta_o = 9$$

Accordingly, this established a minimum radial wall distance, 0.64 inches, for wall location, if there are to be no wall effects. End effects are more nebulous and require more consideration. Since neither this investigation nor those similar studies reported in the literature inquired into this aspect of the problem, the question of, "How far must the sensor be located from the tank end if end effects are to have no effect upon sensor measurements?", must be left unanswered.

5-2. Conclusions

In view of close agreement between theory and experiment which was demonstrated in this study, it is felt that the following objectives have been achieved:

(1) A suitable mathematical model for describing the flow induced by the harmonic oscillation of an infinite cylinder in a viscous medium of infinite extent has been derived theoretically.

(2) The applicability of this model has been confirmed experimentally.

(3) The mathematical model, which was derived for the infinite case, may also be applied to a flow system for finite extent, but with caution.

Since none of this information has been developed by prior studies, it is felt that this investigation has extended the knowledge of time dependent, axisymmetric viscous flows.

5-3. Recommendations for Future Studies

It should not be implied that the results of this investigation in any way complete the work which should be accomplished for the oscillating rod. Areas wherein additional investigative work should be undertaken are discussed in the following paragraphs. The list is not exhaustive, but it is intended to indicate a few possibilities for future research.

The most pressing area wherein additional study is indicated must be a careful investigation into transition to turbulence for the induced flow. This might be best approached by obtaining critical Reynolds numbers for a number of cylinders of different roughness. It would seem that such data could then be extrapolated to zero roughness, to obtain the critical Reynolds number for a smooth rod. Use of a fluid of much lower viscosity, say water, should be considered.

An experimental study of the stability of the induced laminar flow is indicated. In connection with this study, the major problem would be the introduction of a disturbance on the surface of the oscillating rod whose behavior could then be observed as the shear wave was propagated outward from the rod. Amplification or damping of the disturbance would be detected with hot wire equipment by positioning sensors at a number of radial locations in the fluid.

A wide range of studies could be undertaken wherein heat was transferred from the oscillating rod to the fluid. Included should be a theoretical analysis of the temperature profile in the fluid; a study of the effect of temperature dependent fluid properties upon the induced velocity profiles; an investigation into the effect of heat transfer upon the stability of the induced laminar flow; and finally, a determination of the variation of heat transfer coefficients from the rod during the oscillation cycle.

SELECTED BIBLIOGRAPHY

1. Batchelor, G. K. "The Skin Friction on Infinite Cylinders Moving Parallel to their Length." Quarterly Journal of Mechanics, Vol. 7, 1954, pp. 179-192.

2. Combs, G. D. and Gilbrech, D. A. "Pulsating Flow Research." University of Arkansas Research Report Series - No. 4, Fluid Mechanics Research No. 1, 1964.

3. Dryden, H. L., F. P. Murnaghan, and H. Bateman. Hydrodynamics. New York: Dover Publications, Inc., 1956, pp. 155-176.

4. Flugge, W. Four Place Tables of Transcendental Functions. New York: McGraw-Hill Book Co., Inc., 1954, pp. 62-67.

5. Gilmont, R. "A Falling-Ball Viscometer." Instrument and Control Systems, Vol. 36, No. 9, 1963, pp. 121-123.

6. Glauert, M. B. "The Laminar Boundary Layer on Oscillating Plates and Cylinders." Journal of Fluid Mechanics, Vol. 1, No. 1, 1956, pp. 97-110.

7. Grant, H. P. and R. E. Kronauer. "Fundamentals of Hot Wire Anemometry." Symposium on Measurement in Unsteady Flow, American Society of Mechanical Engineers. New York, 1962, pp. 44-53.

8. Hasimoto H. "Rayleigh's Problem for a Cylinder of Arbitrary Shape, II." Journal of the Physical Society of Japan, Vol. 10, 1955, pp. 397-406.

9. Hasimoto H. "The Unsteady Axial Motion of an Infinitely Long Cylinder in a Viscous Fluid." Proceedings of the 9th International Congress of Applied Mechanics, Vol. 3, 1956, pp. 135-144.

10. Hildebrand, F. B. Advanced Calculus for Applications. Englewood Cliffs, New Jersey: Prentice-Hall, Inc., 1965, pp. 149-153 and 181.

11. Hunt, H. N. Incompressible Fluid Dynamics. New York: John Wiley and Sons, Inc., 1964, pp. 54-62.

12. Kreith, F. Principles of Heat Transfer. Scranton, Pennsylvania: International Textbook Co., 1965, pp. 412-414 and p. 598.

13. Laurence, J. C. and V. A. Sandborn. "Heat Transfer from Cylinders." Symposium on Measurement in Unsteady Flow, American Society of Mechanical Engineers, 1962, pp. 36-43.

14. Li, H. "Stability of Oscillatory Laminar Flow Along a Wall." Beach Erosion Board Technical Memorandum No. 47. 1954, pp. 1-35.

15. Lin, C. C. "On the Stability of Two Dimensional Parallel Flows." Quaterly of Applied Mathematics, Number 3, July 1945, pp. 218; January 1946, pp. 277.

16. McLachlan, N. W., and Meyers, A. L. "The Polar Form of the ker and kei Functions with Application to Eddy Current Heating." Seventh Series, October, 1934, pp. 610-624.

17. Moore, F. K. "Unsteady Laminar Boundary Layer Flow." National Advisory Committee for Aeronautics Technical Note 2471, 1951, pp. 1-33.

18. O'Brien, V. and F. E. Logan. "Periodic Boundary Layer Flows Over a Flat Plate." Part II. Applied Physics Laboratory Technical Memorandum TG-658, 1965, pp. 1-82.

19. Rayleigh, Lord. "On the Motion of Solid Bodies Through Viscous Liquids." Philosophical Magazine, Vol. 21, 1911, pp. 697-711.

20. Runstadler, P. W. "Stable Operation of Hot Film Proves in Water." Symposium on Measurement in Unsteady Flow, American Society on Mechanical Engineers, 1962, pp. 83-84.

21. Sarpkaya, T. "Mechanism of Turbulence Generation in Pulsating Viscous Flow." NU-Hydro-Report No. 012-TS, University of Nebraska, 1964.

22. Sarpkaya, T. "Experimental Determination of the Critical Reynolds Number for Pulsating Poiseuille Flow." ASME Paper 66-FE-5, American Society of Mechanical Engineers, 1966.

23. Schlichting, H. Boundary Layer Theory. New York: McGraw-Hill Book Company, Inc., 1955, pp. 72-78 and pp. 207-237.

24. Stuart, J. T. Laminar Boundary Layers, Part VII. Oxford: Oxford University Press, 1963, pp. 349-406.

25. Stewartson, K. "The Theory of Unsteady Laminar Boundary Layers." Advances in Applied Mechanics, Academic Press, Vol. 7, 1956, pp. 1-35.

26. Stokes, G. G. "On the Effect of the Internal Friction of Fluids on the Motion of Pendulums." Transactions of the Cambridge Philosophical Society, Vol. 9, Part II, 1851, pp. 8-106.

27. Watson, E. J. "Boundary Layer Growth." Proceedings of the Royal Society, Series A, Vol. 231, 1955, pp. 104-116.

28. Wills, J. A. B. "The Correction of Hot Wire Readings for Proximity to a Solid Boundary." Journal of Fluid Mechanics, Vol. 12, 1962, pp. 388.

29. Wuest, W. "Boundary Layers on Cylindrical Bodies with Unsteady Axial Motion." Zeitschrift für Angewandte Mathematik und Mechanik, Vol. 32, No. 6, 1952, pp. 172-178.

30. Wylie, C. R. Advanced Engineering Mathematics. New York: McGraw-Hill Book Company, Inc., 1951, pp. 249-288.

APPENDIX A

SENSOR TEMPERATURE INVESTIGATION

$$\text{Power} = I^2R$$
$$= \left(\frac{25}{1000} \right)^2 \quad 1 = \frac{0.625}{1000} \text{ watts}$$
$$= \quad .625\ (.0568) \times 10^{-3} \ \frac{\text{Btu}}{\text{min}}$$

Assume fluid to be a light oil with properties as given by Kreith (12), page 598.

If, as is customary, fluid properties are evaluated at the average of the wire temperature, T_s, and the fluid temperature, T, then for an 80° average fluid temperature

$$N_P = 570 \qquad k = 0.077 \ \frac{\text{Btu}}{\text{hr ft °F}} \qquad \nu = 49 \times 10^{-5} \ \text{ft}^2/\text{sec.}$$

Laurence and Sandborn (13) have indicated that a suitable correlation for heat transfer by forced convection from a wire in cross flow is given by

$$N_N = 0.42\ N_P^{\ 0.2} + 0.57\ N_P^{\ 0.33}\ N_R^{\ 0.5}.$$

Based upon a velocity of 0.5 ft/sec

$$N_R = \frac{DV}{\nu} \quad \frac{.00035}{12} \ \frac{(.5)}{49} \times 10^5$$
$$= \frac{35}{24(49)} \quad = \quad 0.0298$$

and

$$N_R^{\ 0.5} \ = \ \frac{1.729}{10} \ = \ .1729$$

Hence,

$$N_N = .42(570)^{.2} + .57(570)^{.33}(.1729) = 2.29$$

Since

$$h = \frac{k\ N_N}{D} \quad \frac{00.077}{60} \quad \frac{(2.29)}{\frac{(.000.35)}{12}} \qquad \frac{\text{Btu}}{\text{ft}^2\ °\text{F min}}$$

or $\quad h=101 \quad \frac{\text{Btu}}{\text{ft}^2\ °\text{F min}}$

A heat balance for the hot wire requires that

$$I^2R = hA\ (T_s - T).$$

Therefore,

$$.0354 \times 10^{-3} = 101(.336 \times 10^{-6})\ \Delta T$$

$$.354 \times 10^{-4} = 1.01(336 \times 10^{-4})\ \Delta T$$

or $\quad \Delta T = \frac{.354}{.336(1.01)} = 1.04$

Then $\quad T_s = 80 + 1.04 \doteq 81°$

and

$$\frac{T_s + T}{2} = 80.5°$$

which agrees with the assumption made in this analysis.

To be considered "remote from the surface, the sensor should be at least $\frac{5D}{N_N}$ inches away from the surface.

In this case

$$\frac{5D}{N_N} = 5\frac{D}{N_N} = 5\frac{(.00035)}{2.29}$$

$$= 0.00076 \text{ inches}$$

Since the sensor was about one tenth millimeter away from the surface at the closest, the sensor could always be considered as "remote."

APPENDIX B

ERROR ANALYSIS

In evaluating the experimental work performed in this study, consideration should be given to the effect of experimental errors upon the results which were obtained.

This study required the ability to measure the following items: fluid properties, sensor position, and fluid velocity.

It would be expected that the measurement of fluid properties would be reproducible to within 5% with the instrumentation employed. While the specific gravity determination was much better than this, this 5% reproducibility was typical for the viscosity determination.

Sensor position was determined to 0.01 cm with the vernier scale employed. No significant variation in the velocity determination was noted for variation in sensor position of 0.01 cm. In view of this, sensor position did not seem to be a source of significant error.

The major source of experimental error was a result of the inability to accurately determine low fluid velocities. This problem arose as a result of the low sensitivity of the anemometer as well as variation from harmonic rod displacement, due to poor motor performance at low speeds, during sensor calibration. A reasonable estimate of the velocity error could be from 0.1 inches per second to 0.2 inches per second.

APPENDIX C

Tabulated Velocity Data

TABLE I

VELOCITY DATA

Test 62-1

U_o = 162 74° a = 0.25 in.

Rad. Dist. mm	Max. Vel. in/sec	Vel. Factor 0°	45°	90°	Vel. Units in/sec 0°	45°	90°	Vel. Ratio 0°	45°	90°
0	1.62	3/3	2/3	0/3	1.62	1.11	0.0	1.0	.68	0.0
2	.75	$\frac{1.4}{1.5}$	$\frac{1.5}{1.5}$	$\frac{.6}{1.5}$	.70	.75	.3	.43	.46	.18
4	.25	$\frac{0.7}{1}$	$\frac{1}{1}$	$\frac{0.5}{1}$	.175	.25	.125	.11	.15	.08

TABLE II

VELOCITY DATA

Test 62-2

U_o = 1.62 in/sec a = 0.25 in/sec

Rad. Dist. mm	Max. Vel. in/sec	Vel. Factor			Vel. Units in/sec			Vel. Ratio		
		0°	45°	90°	0°	45°	90°	0°	45°	90°
0	1.62	3/3	2/3	0/3	1.62	1.11	0.0	1.0	.68	0.0
2	.75	$\frac{1.4}{1.5}$	$\frac{1.5}{1.5}$	$\frac{.6}{1.5}$	.70	.75	.3	.43	.46	.18
4	.25	$\frac{0.7}{1}$	$\frac{1}{1}$	$\frac{0.5}{1}$	.175	.25	.125	.11	.15	.08

TABLE III

VELOCITY DATA

Test 78-1

U_o = 6.15 in/sec 74° a = 3/4 in.

Rad. Dist. mm	Max. Vel. in/sec	Vel. Factor			Vel. Units in/sec			Vel. Ratio		
		0°	45°	90°	0°	45°	90°	0°	45°	90°
0	6.15	$\frac{10.5}{10.5}$	$\frac{7.5}{10.5}$	$\frac{0.0}{10.5}$	6.15	4.40	0.0	1.0	.71	0.0
2	2.30	$\frac{7.0}{7.5}$	$\frac{7.5}{7.5}$	$\frac{4.1}{7.5}$	2.15	2.30	1.26	.35	.38	.205
4	1.0	$\frac{3.0}{6.0}$	$\frac{6.0}{6.0}$	$\frac{6.0}{6.0}$	.5	1.0	1.0	.18	.16	.16
6	0.5	$\frac{0.0}{4.0}$	$\frac{3.5}{4.0}$	$\frac{4.0}{4.0}$	0.0	.44	.50	0.0	.07	.08
8	0.3	$\frac{-1.0}{2.5}$	$\frac{0.5}{2.5}$	$\frac{2.0}{2.5}$	-.12	.12	.24	-.02	+.02	+.04

TABLE IV

VELOCITY DATA

Test 78-2

U_o = 6.15 in/sec 75° a= 3/4 in.

Rad. Dist. mm	Max. Vel. in/sec	Vel. Factor 0°	Vel. Factor 45°	Vel. Factor 90°	Vel. Units in/sec 0°	Vel. Units in/sec 45°	Vel. Units in/sec 90°	Vel. Ratio 0°	Vel. Ratio 45°	Vel. Ratio 90°
0	6.15	$\frac{11.0}{11.0}$	$\frac{7.5}{11.0}$	$\frac{0.0}{11.0}$	6.15	4.19	0.0	1.0	.68	0.0
2	2.30	$\frac{7.0}{7.5}$	$\frac{7.5}{7.5}$	$\frac{4.0}{7.5}$	2.15	2.30	1.23	.35	.38	.20
4	1.0	$\frac{3.0}{6.0}$	$\frac{6.0}{6.0}$	$\frac{6.0}{6.0}$	.5	1.0	1.0	.08	.16	.16
6	0.5	$\frac{0.0}{4.0}$	$\frac{3.5}{4.0}$	$\frac{4.0}{4.0}$	0.0	.44	.50	0.0	.07	.08
8	0.3	$\frac{-.7}{2.0}$	$\frac{0.7}{2.0}$	$\frac{1.5}{2.0}$	-.105	+.105	.225	-.017	.017	+.036

TABLE V

VELOCITY DATA

Test 78-3

U_o = 6.15 in/sec   75°   a = 3/4 in.

Rad. Dist. mm	Max. Vel. in/sec	Vel. Factor 0°	Vel. Factor 45°	Vel. Factor 90°	Vel. Units in/sec 0°	Vel. Units in/sec 45°	Vel. Units in/sec 90°	Vel. Ratio 0°	Vel. Ratio 45°	Vel. Ratio 90°
0	6.15	$\frac{10.0}{10.0}$	$\frac{7.0}{10.0}$	$\frac{0.0}{10.0}$	6.15	4.31	0.0	1.0	0.7	0.0
2	2.30	$\frac{7.0}{7.5}$	$\frac{7.5}{7.5}$	$\frac{4.0}{7.5}$	2.15	2.30	1.23	.35	.38	.20
4	1.0	$\frac{3.0}{6.0}$	$\frac{6.0}{6.0}$	$\frac{6.0}{6.0}$	0.5	1.0	1.0	.08	.16	.16
6	0.5	$\underline{0.0}$	$\frac{3.5}{4.0}$	$\frac{4.0}{4.0}$	0.0	0.44	0.50	0.0	.07	.08
8	0.3	$\frac{-.8}{2.0}$	$\frac{0.8}{2.0}$	$\frac{1.5}{2.0}$	-.12	+.12	0.225	-.019	+.019	+.036

TABLE VI

VELOCITY DATA

Test 78-4

U_o = 6.15 in/sec 73° a = 3/4 in.

Rad. Dist. mm	Max. Vel. in/sec	Vel. Factor 0°	Vel. Factor 45°	Vel. Factor 90°	Vel. Units in/sec 0°	Vel. Units in/sec 45°	Vel. Units in/sec 90°	Vel. Ratio 0°	Vel. Ratio 45°	Vel. Ratio 90°
0	6.15	$\frac{10.0}{10.0}$	$\frac{7.0}{10.0}$	$\frac{0.0}{10.0}$	6.15	4.31	0.0	1.0	7.0	0.0
2	2.30	$\frac{7.0}{7.5}$	$\frac{7.5}{7.5}$	$\frac{4.0}{7.5}$	2.15	2.30	1.23	.35	.38	.30
4	1.0	$\frac{3.0}{6.0}$	$\frac{6.0}{6.0}$	$\frac{6.0}{6.0}$	0.5	1.0	1.0	.08	.16	.16
6	0.5	$\frac{0.0}{4.0}$	$\frac{3.5}{4.0}$	$\frac{4.0}{4.0}$	0.0	0.44	0.50	0.00	0.07	0.08
8	0.3	$\frac{-.8}{2.0}$	$\frac{0.8}{2.0}$	$\frac{1.5}{2.0}$	-.12	+.12	0.225	-.019	+.019	+.36

TABLE VII

VELOCITY DATA

Test 268-1

U_o = 7.03 in/sec 75° a = 1/4 in.

Rad. Dist. mm	Max. Vel. in/sec	Scale Factor 0°	45°	90°	Vel. Units in/sec 0°	45°	90°	Vel. Ratio 0°	45°	90°
0	7.03	2.0/2.0	1.4/2.0	0.0/2.0	7.04	4.95	0.0	1	.07	0.0
1	5.5	1.5/2.0	1.6/2.0	1.8/2.0	4.13	4.4	2.20	.59	.63	.31
2	1.6	1.5/2.0	2.0/2.0	1.8/2.0	1.2	1.6	1.4	.17	.22	.21
3	1.0	0.0/1.5	1.0/1.5	1.2/1.5	0.0	.67	.8	0.0	.09	.11
4	0.6	-.5/1.0	+.5/1.0	1.0/1.0	-.3	.3	.6	-.04	+.04	+.08
5	0.3	-.8/1.0	0.0/1.0	+.5/1.0	-.24	0.0	.15	-.03	0.0	+.02

TABLE VIII

VELOCITY DATA

Test 268-2

U_0 = 7.03 in/sec   75°   a = 1/4 in.

Rad. Dist. mm	Max. Vel. in/sec	Scale Factor 0°	45°	90°	Vel. Units in/sec 0°	45°	90°	Vel. Ratio 0°	45°	90°
0	7.03	$\frac{2.0}{2.0}$	$\frac{1.4}{2.0}$	$\frac{0.0}{2.0}$	7.04	4.95	0.0	1.0	.7	0.0
1	5.5	$\frac{1.6}{2.0}$	$\frac{1.7}{2.0}$	$\frac{1.8}{2.0}$	4.4	4.67	2.20	.62	.67	.31
2	1.6	$\frac{1.5}{2.0}$	$\frac{2.0}{2.0}$	$\frac{1.8}{2.0}$	1.2	1.6	1.44	.17	.22	.21
3	1.0	$\frac{0.0}{1.2}$	$\frac{0.8}{1.2}$	$\frac{1.0}{1.2}$	0.0	.67	.86	0.0	.09	.12
4	0.6	$\frac{-.5}{1.0}$	$\frac{+.5}{1.0}$	$\frac{1.0}{1.0}$	-.3	+.3	+.6	-.04	+.04	+.08
5	0.3	$\frac{-.8}{0.9}$	$\frac{0.0}{0.9}$	$\frac{+.5}{0.9}$	-.267	0.0	.167	-.04	0.00	+.02

TABLE IX

VELOCITY DATA

Test 268-3

U_o = 7.03 in/sec 75° a = 1/4 in.

Rad. Dist. mm	Max. Vel. in/sec	Scale Factor 0°	45°	90°	Vel. Units in/sec 0°	45°	90°	Vel. Ratio 0°	45°	90°
0	7.03	$\frac{2.0}{2.0}$	$\frac{1.4}{2.0}$	$\frac{0.0}{2.0}$	7.03	4.95	0.0	1.0	.7	0.0
1	5.50	$\frac{1.6}{2.0}$	$\frac{1.7}{2.0}$	$\frac{0.8}{2.0}$	4.4	4.67	2.20	.62	.67	.31
2	1.60	$\frac{1.0}{1.5}$	$\frac{1.5}{1.5}$	$\frac{1.2}{1.5}$	1.07	1.6	1.28	.15	.22	.18
3	1.0	$\frac{0.0}{1.2}$	$\frac{0.8}{1.2}$	$\frac{0.9}{1.2}$	0.0	.66	.75	0.00	.09	.11
4	0.6	$\frac{-.4}{1.0}$	$\frac{+.4}{1.0}$	$\frac{+.5}{1.0}$	.24	+.24	.6	-.03	+.03	+.08
5	0.3	$\frac{-.6}{0.9}$	$\frac{0.0}{0.9}$	$\frac{+.5}{0.9}$	-.2	0.0	.167	-.03	0.0	+.02

TABLE X

VELOCITY DATA

Test 268-4

U_o = 7.03 in/sec 75° a = 1/4 in.

Rad. Dist. mm	Max. Vel. in/sec	Scale Factor 0°	45°	90°	Velocity Units in/sec 0°	45°	90°	Velocity Ratio 0°	45°	90°
0	7.03	$\frac{2.0}{2.0}$	$\frac{1.4}{2.0}$	$\frac{1.0}{2.0}$	7.13	4.95	0.0	1.0	.7	0.0
1	5.50	$\frac{1.4}{2.0}$	$\frac{1.7}{2.0}$	$\frac{0.8}{2.0}$	3.84	4.67	2.20	.55	.67	.31
2	1.6	$\frac{1.5}{2.0}$	$\frac{2.0}{2.0}$	$\frac{1.8}{2.0}$	1.2	1.6	1.44	.17	.22	.21
3	1.0	$\frac{0.0}{1.2}$	$\frac{0.8}{1.2}$	$\frac{0.9}{1.2}$	0.0	.66	.75	0.0	.09	.11
4	0.6	$\frac{-.5}{1.0}$	$\frac{+.5}{1.0}$	$\frac{1.0}{1.0}$	-.3	+.3	.6	-.04	+.04	.08
5	0.3	$\frac{-.8}{0.9}$	$\frac{0.0}{0.9}$	$\frac{+.5}{0.9}$	-.267	0.0	.167	-.04	0.00	+.02

TABLE XI

VELOCITY DATA

Test 268-5

U_o = 14.5 in/sec 78° a = 0.5 in.

Rad. Dist. mm	Max. Vel. in/sec	Scale Factor			Velocity Units in/sec			Velocity Ratio		
		0°	45°	90°	0°	45°	90°	0°	45°	90°
0	14.5	$\frac{3.4}{3.4}$	$\frac{2.4}{3.4}$	$\frac{0.0}{3.4}$	14.5	10.25	0.0	1.0	.70	0.0
1	11.5	$\frac{2.8}{3.2}$	$\frac{2.9}{3.2}$	$\frac{1.4}{3.2}$	9.19	9.52	4.6	.635	.66	.32
2	5.3	$\frac{2.5}{3.2}$	$\frac{3.2}{3.2}$	$\frac{2.7}{3.2}$	4.15	5.3	4.47	.29	.36	.30
3	3.0	$\frac{0.5}{2.5}$	$\frac{1.5}{2.5}$	$\frac{1.8}{2.5}$	0.6	1.8	2.16	.04	.12	.15
4	2.1	$\frac{-1.0}{2,5}$	$\frac{0.5}{2,5}$	$\frac{-1.0}{2,5}$	-.84	.42	.84	-.06	+.13	-.06
5	1.0	$\frac{-0.8}{1.0}$	$\frac{-0.4}{1.0}$	$\frac{-0.8}{1.0}$	-.8	-.4	+.8	-.05	-.03	+.05
6	0.2	$\frac{-1.0}{1.0}$	$\frac{-0.5}{1.0}$	$\frac{-0.5}{1.0}$	-.2	-.1	-.1	-.01	-.01	-.01

TABLE XII

VELOCITY DATA

Test 268-6

U_o = 14.5 in/sec 74° a = 0.5 in.

Rad. Dist. mm	Max. Vel. in/sec	Scale Factor 0°	45°	90°	Velocity Units in/sec 0°	45°	90°	Velocity Ratio 0°	45°	90°
0	14.5	$\frac{3.4}{3.4}$	$\frac{2.4}{3.4}$	$\frac{0.0}{3.4}$	14.5	10.25	0.0	1.0	0.7	0.0
1	10.5	$\frac{2.8}{3.2}$	$\frac{2.0}{3.2}$	$\frac{1.4}{3.2}$	9.19	9.52	4.6	.64	.66	.32
2	5.3	$\frac{2.5}{3.2}$	$\frac{3.2}{3.2}$	$\frac{2.7}{3.2}$	4.15	5.3	4.47	.29	.36	.30
3	3.0	$\frac{0.5}{2.5}$	$\frac{1.5}{2.5}$	$\frac{1.8}{2.5}$	0.6	1.8	2.16	.04	.12	.15
4	2.1	$\frac{-1.0}{2.5}$	$\frac{0.5}{2.5}$	$\frac{1.0}{2.5}$	-.84	+.42	2.2	-.06	+.03	+.06
5	1.0	$\frac{-0.8}{1.0}$	$\frac{-0.4}{1.0}$	$\frac{0.8}{1.0}$	-.8	-.4	+.8	-.05	-.03	+.05
6	0.2	$\frac{-1.0}{1.0}$	$\frac{-0.5}{1.0}$	$\frac{-0.5}{1.0}$	-.2	-.1	-.1	-.01	-.01	-.01

TABLE XIII

VELOCITY DATA

Test 268-7

U_o = 14.5 in/sec | 75° | a = 1.5 in.

Rad. Dist. mm	Max. Vel. in/sec	Scale Factor 0°	45°	90°	Velocity Units in/sec 0°	45°	90°	Velocity Ratio 0°	45°	90°
0	14.5	$\frac{3.3}{3.3}$	$\frac{2.3}{3.3}$	$\frac{0.0}{3.3}$	14.5	10.2	0.0	1.0	.69	0.0
1	10.5	$\frac{2.9}{3.3}$	$\frac{3.0}{3.3}$	$\frac{1.5}{3.3}$	9.22	9.55	4.77	.64	.66	.33
2	5.3	$\frac{2.4}{3.0}$	$\frac{3.0}{3.0}$	$\frac{2.5}{3.0}$	4.24	5.3	4.41	.29	.36	.30
3	3.0	$\frac{0.6}{2.2}$	$\frac{1.5}{2.2}$	$\frac{1.8}{2.2}$	.819	2.15	2.46	.06	.14	.17
4	2.1	$\frac{-0.4}{1.0}$	$\frac{+0.2}{1.0}$	$\frac{+0.4}{1.0}$	-.81	+.42	.84	-.06	+.03	+.06
5	1.0	$\frac{-0.8}{1.0}$	$\frac{-0.4}{1.0}$	$\frac{+0.8}{1.0}$	-.8	-.4	+.8	-.05	-.03	+.05
6	0.2	$\frac{-1.0}{1.0}$	$\frac{-0.5}{1.0}$	$\frac{-0.5}{1.0}$	-.2	-.1	-.1	-.01	-.01	-.01

VITA

John Edward Kipp

Candidate for the Degree of

Doctor of Philosophy

Thesis: STOKES' PROBLEM FOR THE INFINITE ROD

Major Field: Engineering

Biographical:

Personal Data: Born January 5, 1930, in Lincoln, Nebraska, the son of Harold L. and Constance A. Kipp.

Education: Attended grade school and high school in Lubbock, Texas; graduated from Lubbock High School in May, 1947; received the Bachelor of Science degree in Mechanical Engineering from the University of Kansas in June, 1951; received the Master of Science degree from the University of Kansas with a major in Mechanical Engineering in June, 1955; completed the requirement for the degree of Doctor of Philosophy in May, 1968.

Professional Experience: Entered the United States Air Force in 1951 and served until 1953 as a Communications and Cryptographic Officer; associated with the University of Kansas as an Instructor, Department of Applied Mechanics from 1953 to 1956; employed by Kansas State University as Assistant Professor of Applied Mechanics from 1956 to 1963; received Science Faculty Fellowship from the National Science Foundation for study at Oklahoma State University during the period June, 1963 to September 1964; employed by Kansas State University as Assistant Professor of Applied Mechanics from September, 1964 to June, 1968.

Professional Organizations: Registered Professional Engineer in Kansas. Member of Pi Tau Sigma, Sigma Tau, Pi Mu Epsilon, and American Society for Engineering Education. Associate Member of American Society of Mechanical Engineers.